Impact of warming on functional traits of a keystone grazer in Arctic lakes

Athina Karapli-Petritsopoulou[1,2*], Dörthe Becker[3], Dagmar Frisch[1]

[1] Department of Evolutionary and Integrative Ecology, Leibniz Institute of Freshwater Ecology and Inland Fisheries (IGB), Berlin, Germany

[2] Department of Biology, Chemistry, Pharmacy, Institute of Biology, Freie Universität Berlin, Berlin, Germany

[3] NABU-Naturschutzstation Niederrhein, Kleve, Germany

*Corresponding author: athena.karapli@igb-berlin.de

Keywords: thermal stress; *Daphnia*; Haemoglobin; Glutathione-S-transferase; Lipid peroxidation; life history

Abstract

Temperature rise is one of the most pronounced abiotic changes currently affecting Arctic ecosystems. Knowledge about the adaptation capacity of their key species is urgently needed to better understand the ecological consequences for these sentinel ecosystems. Previous work on a keystone zooplankton grazer, the obligatory parthenogenetic *Daphnia pulicaria*, from a lake in South-West Greenland revealed a decreased thermal tolerance over the course of a decade. To assess its thermal responses in more detail, we compared physiological and life history traits of four clones from the same population that originate from two time periods a decade apart. The tested clones represent two closely related genetic clusters. Both were present in the 2022 population, but only one was present also in 2011. Two of the clones were previously resurrected from the sediment dating to ca. 2011. We tested three temperatures to reflect future climate warming scenarios: 14°C, 16°C, and 18°C. The tested temperature range did not alter most of the measured traits, but there were pronounced differences between clones at all temperatures. Results indicated that genetic cluster membership, rather than time period of origin, determined the clones' responses. The clone representing the genetic cluster detected only in 2022 had consistently higher stress and lower fitness across all tested temperatures. To better understand the implications for the lake ecosystem, a more comprehensive survey of clonal diversity and the survival capacity of additional clones present in the population under projected warming scenarios is needed.

Introduction

Arctic freshwater ecosystems are experiencing some of the fastest environmental alterations driven by a complex interplay of multiple factors (Prowse et al. 2006; Anderson et al. 2017; Saros et al. 2025). A key member of those ecosystems is the keystone grazer *Daphnia*, a microcrustacean that due to its multiple ecological interactions can serve as a sentinel for ecosystem impacts (Altshuler et al. 2011; Miner et al. 2012). *Daphnia* is an excellent eco-evolutionary model, exemplified by its eco-responsiveness and potential for rapid adaptation. A multitude of studies have tested aspects regarding its physiology, genome, transcriptome and ecology (Lampert 2011; Ebert 2022). Arctic *Daphnia* are often polyploid and obligately parthenogenetic (Innes and Dufresne 2020) and are poorly studied compared with their temperate con-specifics (but see Weider and Hebert 1987; Dufresne and Hebert 1997; Colbourne et al. 1998; Weider et al. 1999; Przytulska et al. 2015; Pecl et al. 2025). Studying physiological traits of Arctic *Daphnia* populations in response to relevant environmental factors such as temperature can serve as a starting point both for monitoring the impacts of rapid environmental change on their respective lake systems and for answering questions related to the rapid adaptation capacity of parthenogens.

The effects of thermal stress and linked rapid adaptation capacity have been the focus of recent research in light of anthropogenic climate change and global warming (Catullo et al. 2019). Thermal sensitivity is often assessed at the species level in an effort to predict vulnerability to warming and, by extension, to climate change (Bennett et al. 2019). However, phenotypic plasticity, variation between and within populations, local adaptation, and multifactorial environmental pressures need to be considered as all these aspects shape each population's physiological profile (Chown et al. 2010; Bennett et al. 2019). Assessing upper thermal limits is useful for a first assessment of an organism's thermal tolerance (Geerts et al. 2015; Burton et al. 2018). As a next step, biomarkers related to oxidative stress, antioxidant defence, oxygen transfer and capacity, and life history traits are important for a deeper understanding of the physiological effects of thermal stress.

One of the primary limiting factors for thermal tolerance is its link to oxygen transfer and capacity (Pörtner 2001, 2002, 2010). Especially for water-breathers, warmer temperatures result in lower oxygen solubility, and hence lower oxygen supply. As metabolic rates are higher at elevated temperatures, oxygen demand also increases (Khan and Khan 2008; Kielland et al. 2019). Higher metabolic rates can also lead to a higher production of radical oxygen species (ROS), breaking the balance between ROS production and elimination, thus causing oxidative stress (Lushchak 2011; Pamplona and Costantini 2011). The elimination of ROS is performed by antioxidant mechanisms involving enzymes like glutathione-S-transferases, glutathione peroxidase, catalase or superoxide dismutase (Barata et al. 2005b; Bae et al. 2016). If the antioxidant systems can be efficiently upregulated in response to oxidative stress, they will restore the balance and return the organism to its normal physiological state (Lushchak 2011). However, if the antioxidant mechanisms are inefficient, the levels of oxidative damage caused by ROS will increase, resulting in tissue and biomolecule damage including higher levels of lipid peroxidation (the oxidation of membrane fatty acids; Barata et al. 2005a; Pamplona and Costantini 2011).

Thermal stress physiology in *Daphnia* has been extensively studied (e.g., Lamkemeyer et al. 2003; Paul et al. 2004; Schwerin et al. 2009; Becker et al. 2011, 2018; Yampolsky et al. 2014; Coggins et al. 2017; Im et al. 2020; Samanta et al. 2020; Zeis et al. 2023). Responses after exposure to warmer temperatures include increased oxygen consumption, combined with higher limb movement and heart rate (Paul et al. 1997; Lamkemeyer et al. 2003). When the thermal stress persists or the animals are acclimated to a higher temperature, haemoglobin (Hb) concentration increases (Lamkemeyer et al. 2003; Zeis et al. 2013; Cuenca Cambronero et al. 2018) and the antioxidant defence systems are activated (Becker et al. 2011; Bae et al. 2016; Coggins et al. 2017). Elevated lipid peroxidation, indicative of oxidative damage, has been reported as a consequence of thermal stress (Zeis et al. 2019; Samanta et al. 2020). Naturally, temperature changes do not only affect biochemical processes, but are also reflected at the life history level: *Daphnia* reared at higher

92 temperatures mature earlier and achieve smaller body sizes, as well as faster growth rate to
93 maturity (Bae et al. 2016; Hoefnagel et al. 2018; Im et al. 2020a).

94 A powerful tool to assess populations' responses across time related to environmental change is the
95 method of resurrection ecology, where resting stages can be hatched from dated sediment and be
96 tested for the traits of interest (Weider et al. 2018). Previous studies using resurrection ecology on
97 *Daphnia* have demonstrated various rapid responses, for example related to rising temperatures
98 (Geerts et al. 2015; Cuenca Cambronero et al. 2018; Yousey et al. 2018), eutrophication (Hairston et
99 al. 1999; Frisch et al. 2014), ultraviolet radiation (Oexle et al. 2016) and salinisation (Wersebe and
100 Weider 2023). However, none of these studies have involved polyploid, obligate parthenogens.

101 Here, we aim to assess the stress that temperature increase would impose on current and past
102 genotypes representing the Arctic *Daphnia pulicaria* Braya Sø lake population in South-West
103 Greenland. These *Daphnia* are triploid obligate parthenogens (OP) (Karapli-Petritsopoulou et al.
104 2025a). Previous work found a higher thermal and hypoxia tolerance in historical clones hatched
105 from the sediment, dated to ca. 2011 in comparison to modern clones, sampled from the water
106 column in 2022 (for details see Karapli-Petritsopoulou et al. 2025b). In this study, we tested the
107 physiological and life history responses of four clones originating from the two time points (i.e.
108 temporal subpopulations) in response to temperatures reflecting future climate scenarios. For this
109 we quantified three biomarkers: haemoglobin (Hb), lipid peroxidation, and glutathione-S-transferase
110 (GST) activity, known to play a pivotal role in temperature responses of *Daphnia* as detailed above.
111 We also measured the life history traits of growth rate to maturity (GR_{mat}), time to maturity
112 ($Time_{mat}$), and size at maturity ($Size_{mat}$).

113 We expected that elevated temperatures would cause thermal stress in all clones, but especially in
114 the modern clones which have lower thermal and hypoxia tolerance than the historical ones
115 (Karapli-Petritsopoulou et al. 2025b). We therefore hypothesised that all three biomarkers would
116 increase with temperature and that this increase would be higher in the modern, more stressed

Daphnia clones. Similarly, growth rate would increase with temperature in all clones, but the more stressed modern ones would have a slower growth rate and mature later compared with the historical clones, as a consequence of a possible trade-off between oxidative stress and growth or reproduction (Smith et al. 2016; Im et al. 2020b).

Methods

Clonal cultures

This study used Arctic *Daphnia pulicaria* from the oligotrophic, meromictic lake Braya Sø (N66.98785° W051.04123°) near Kangerlussuaq in South-West Greenland (Dane et al. 2020; Karapli-Petritsopoulou et al. 2025a). Laboratory cultures of isofemale lineages (in this work termed "clones") were established either from resurrected individuals or from active single females (Karapli-Petritsopoulou et al. 2025b). In brief, clonal cultures were established from individual adults sampled in the water column of Braya Sø in August 2022. These clones represent the 2022 temporal subpopulation of the lake, termed “modern subpopulation”. The earlier temporal subpopulation, termed “historical subpopulation”, included individuals hatched from single ephippia extracted from sediment dated to ca. 2011, using only one egg per ephippium (for details on dating see Karapli-Petritsopoulou et al. 2025b). Here we used four clones of which two (clones 32 and 5) were resurrected from the sediment (historical subpopulation) and two (clones L9 and L11) originated from the water column (modern subpopulation). Whole genome sequencing revealed that resurrected clones 32 and 5, as well as modern clone L9 belonged to a single genetic cluster (“mixed”) detected in both time periods, while L11 belonged to a genetic cluster (“modern”) specific to the modern population (Fig. 1a; Karapli-Petritsopoulou et al. 2025b).

Synchronisation

All clones had been cultured in common garden conditions at 14°C under 24 hours dimmed light for at least one year (at least 12 asexual generations) prior to this experiment. Cultures were fed with 1 mg C L^{-1} of *Tetradesmus obliquus* (Turpin) M.J. Wynne, 2016 three times a week both before and

during the experiment. The experimental animals were third generation juveniles of clutches 2-6. They originated from juveniles picked from upscaled lab cultures which constituted the grandmaternal generation. Because the Arctic *Daphnia pulicaria* used in this study grow very slowly and produce small clutches with one to five subitaneous eggs, full synchronisation of clutch release of mothers was impossible. Because of this low fecundity, the experiment was performed in overlapping blocks with each experimental unit entering the experiment when there were enough juveniles for at least one replicate.

Experimental design

To quantify the response of each clone to a range of temperatures that reflect future climate warming scenarios, we ran experiments at 14°C, 16°C and 18°C (see Fig. 1 for experimental design schematic). We used physiological assays to measure biomarkers indicative of thermal stress: haemoglobin (Hb) level, thiobarbituric acid-reactive substances (TBARS) as a proxy for lipid peroxidation and Glutathione-S-Transferase (GST) activity as a marker for antioxidant defence (Becker et al. 2011; Cuenca Cambronero et al. 2018; Zeis et al. 2019). Fitness traits that were recorded in response to temperature increase were juvenile mortality, growth rate to maturity (GR_{mat}), time to maturity ($Time_{mat}$), and size at maturity ($Size_{mat}$).

For each clone, juveniles released within 48 hours per clone were pooled before assigning them to replicates, to achieve a random mixture of clutch number and mother origin. Experimental jars were inserted into transparent boxes within one of three incubators (Pol-Eko-Aparatura ST Smart, 430 x 300 x 360 mm, Poland) set to the respective temperature. Incubators were equipped with a dimmed light at the top of the chamber, achieving a light intensity between 20-43 Lux depending on position. For this reason, the position of the boxes within each incubator was randomly changed daily. The experiment was completed within 2.5 months and comprised of 30 overlapping blocks with unbalanced numbers of replicates. Experimental block effects were accounted for in the statistical analysis.

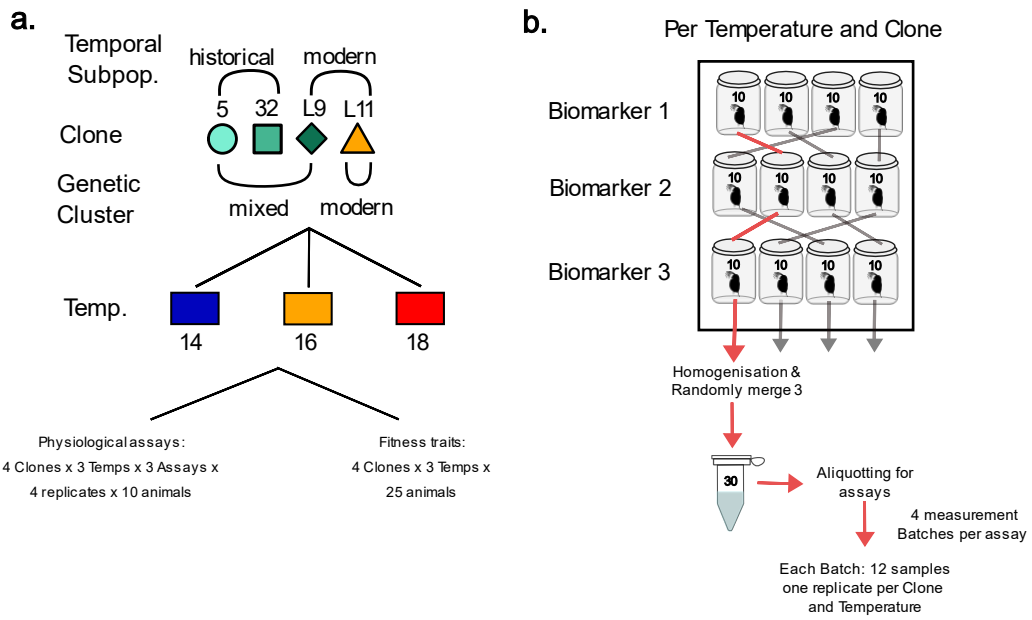

Figure 1. Experimental design schematic representation. Experiment overview (a.) and physiological assay measurement scheme including random merging into four pooled replicates per temperature and clone, aliquoting for each assay and measurement in 4 Batches (b).

Experimental design for physiological assays

Per clone, four replicates containing 10 animals each were exposed to 14°C, 16°C and 18°C, separately for each of the three biomarkers (12 replicates per clone and temperature). For easier monitoring, each replicate of 10 animals was split into two 80 ml jars of five animals in the same box but pooled later again before analysis. Juveniles were grown for 20 days in their respective treatment. On the 10th day of the incubation, juveniles were quickly checked under the stereoscope for the presence of males and were then transferred to fresh medium, removing any males present. On the 20th day, the two jars of five animals were merged again into a single sample, flash-frozen in liquid nitrogen and stored at -80°C until further processing. Jars with lower animal numbers due to mortality or the removal of males were still merged and flash-frozen as long as the final merged sample contained at least five animals. During the 20 days, mortality and maturity (defined here as

the appearance of eggs in the brood chamber) were recorded daily, and any released juveniles were removed.

Experimental design for fitness

To estimate fitness, 25 juveniles per combination of clone and temperature were split randomly into five 80 ml jars containing five individuals each. The jars were monitored daily for mortality and maturity (defined as above). $Time_{mat}$ was recorded, mature animals removed from the jar, and photographed using a dissecting scope (STEMI 508, ZEISS, Germany) at a magnification of 25x. Body length of mature females ($Size_{mat}$) was measured with the image analysis software MikroLive v.5 (https://www.mikroskopie.de/) from the top of the head above the eye to the ventral base of the apical spine in µm. Mature animals were no longer monitored. Jars were checked for male presence on the 10^{th} day of the experiment and any males were removed. The medium was changed on the same day and every 10 days thereafter until all individuals of a jar had matured.

An average 0-day body length baseline of juveniles released within 48 hours was estimated by measuring 20 juveniles per clone. These juveniles did not participate in the experiment. These per-clone baseline averages were used to calculate GR_{mat} as ($Size_{mat}$ – clone baseline)/ $Time_{mat}$.

Physiological assays

To allow measuring of all three biomarkers on the same pools of animals, we randomly merged three replicates per clone and temperature (after tissue homogenisation, see below), yielding four final replicates pooled from the available 12 replicates per clone and temperature with a total number of 30 animals per pooled replicate and then aliquoted for each of the three assays (Fig. 1b). In addition to the assays of Hb, TBARS and GST, we measured total protein content using the Bradford method (Bradford, 1976) for standardisation of each sample. Measurements for each assay were performed in four batches with 12 samples each, comprising of one replicate per clone and temperature.

Aliquoting for three biomarkers

Before pooling, four mini cOmplete™ EDTA-free protease inhibitor cocktail (Roche, Germany) pellets were diluted in 6 ml Phosphate-buffered saline pH 7.4 (PBS; Cold Spring Harbor, 2006) and 100 µl were added to each of the frozen tubes. The tissue was homogenised using Bel-Art® polypropylene pestles. After merging, each pooled replicate contained 300 µl of homogenate. From this, an aliquot of 170 µl was taken for Hb quantification, while the rest was diluted by adding further 150 µl of PBS and mixed by pipetting. The dilution step was necessary to achieve the volume needed for all assays while the Hb aliquot needed to be undiluted due to the low haemoglobin concentration of our samples. Following dilution, two technical replicates of 100 µl were taken for measuring TBARS. The remaining sample was centrifuged at 13000 rpm at 4°C for 10 min. Finally, the supernatant was separated into an aliquot of 40 µl for GST and 25 µl for performing the Bradford assay used for standardising TBARS and GST. For Hb standardisation, total protein was measured from the same supernatant used for Hb. All aliquots were stored in -80°C until further processing, which was completed within 2 days for all assays of each batch. All work was performed on ice. For all blanks and dilutions of reagents, we used the same mixture of PBS and protease inhibitor.

Biomarker quantification

Each measurement batch and assay had its own triplicate standard curve which was used for quantification of the respective batch. All measurements were used to estimate the respective concentrations in the initial sample by considering all dilutions. The estimated concentrations were divided by the sample's total protein content.

Quantification of Hb followed Yampolsky et al. (2014). The respective aliquot was centrifuged at 14000 rpm at 4°C for 10 min and the supernatant transferred to a flat-bottom transparent 96-well plate (Greiner BIO-ONE, Germany), with 50 µl per well and three technical replicates per sample. The absorption spectrum from 230 to 660 nm at 2 nm intervals was measured with a Spark microplate reader (TECAN, Switzerland). Blanks and a standard curve using commercial Haemoglobin from

bovine blood (Sigma-Aldrich) were included for further quantification. Next, 5 µl of each sample and technical replicate were transferred to a new plate and mixed with 95 µl Bradford solution (PanReac AppliChem, Germany) for total protein measurement. Additionally, a standard curve using commercial Bovine Serum Albumin (Sigma-Aldrich, Germany) was constructed for quantification. Absorbance was measured at 595 nm.

From the measured absorbance spectrum of haemoglobin, the average of the blank measurements was subtracted for each measurement batch. We averaged the absorbance of the three technical replicates and quantified total haeme-containing proteins from the Soret peak at 414 nm (Sugano and Hoshi 1971; Zeis 2020) using the standard curve. Following Yampolsky et al. 2014 we calculated the relative oxygenated peaks of haemoglobin at 540 nm and 576 nm as $rPeak_{540} = A_{540} - (A_{520} + A_{560})/2$ and $rPeak_{576} = A_{576} - (A_{560} + A_{600})/2$, respectively. All final calculations were multiplied by initial sample volume and divided by the total protein measured from the same supernatant.

TBARS was measured following the method by Ohkawa et al. (1979). The two TBARS aliquots were mixed with 400 µl of a reaction mix each, made from 10% Acetic acid (final concentration 1.56M), 2-Thiobarbituric acid (final concentration 22.8 M), and 10% sodium dodecyl sulfate (SDS; final concentration 17mM) and incubated for 1h at 95°C. The triplicate standard curve incubated at the same time was constructed using 1,1,3,3-tetramethoxypropane (TMOP; Sigma-Aldrich, Germany). After incubation, tubes were centrifuged at 13000 rpm for 20 min and transferred to transparent 96-well plates. The two TBARS aliquots were split further into four technical replicates per sample. Absorbance was measured at 532 nm with the same microplate reader.

For the quantification of TBARS we used the slope of the TMOP standard curve after setting the intercept to 0. After subtracting the blanks, the average absorbance of the technical replicates per sample was multiplied by the dilution factor and initial sample volume and divided by the standard

curve slope and the total protein per sample. TBARS level was expressed as nmol Malondialdehyde (MDA) per mg protein.

Glutathione-S-transferase activity (GST) was measured using the monochlorobimane (MCB) fluorometric method modified from Nauen and Stumpf (2002). In non-transparent 96-well plates (Greiner BIO-ONE, Germany), 10 µl of the samples were mixed with 100 µl of 500 µM MCB solution, 40 µl PBS buffer, and 100 µl of 100 µM reduced glutathione (GSH; Sigma-Aldrich, Germany) dissolved in PBS buffer. MCB (Synchem, Germany) was first dissolved in dimethyl sulfoxide (DMSO; Agilent, Germany) and then diluted with PBS buffer. Commercial Glutathione-S-transferase from equine liver (GST; Sigma-Aldrich, Germany) was used instead of sample as positive control at a dilution of 1:100 of a 1mg/ml PBS:Glycerin 1:1 stock solution. The fluorescence intensity (Excitation at 355 nm, Emission at 460 nm) was measured with the microplate reader for five minutes starting right after the injection of the GSH solution, with measurement per sample set every 30 seconds. For the standard curve we used the same mixture, replacing the sample with 10 µl commercial GST at a 1:10 dilution of the stock solution, and using varying concentrations of the GSH solution from 0 to 100 µM. The plate was then incubated in the dark for 1 h before measuring Fluorescence intensity.

For GST activity, the slope of the fluorescence change per minute was estimated from the three technical replicates and was divided by the standard curve slope (corresponding to fluorescence per µmol/L GSH) to estimate the substrate conjugation per minute (µmol min^{-1} mg $protein^{-1}$). Finally, the enzyme activity was multiplied by the dilution factor and start volume and divided by the total protein per sample. GST activity was expressed in U/mg protein, where U equals substrate µmol conjugate min^{-1}.

Total protein of the diluted TBARS and GST samples (see above *Aliquoting for three biomarkers*) was performed according to Bradford (1976) as described for the Hb aliquot and was used for the standardisation of the TBARS and GST activity measurements.

Two pooled replicates (one for clone L11 in the 16°C treatment and one for clone L9 at 18°C) were excluded from further analysis due to pipetting errors during homogenisation. These clone/temperature combinations therefore only had three pooled replicates.

Statistical analysis

Linear mixed models were fitted with the lmerTest package (v. 3.1-3; Kuznetsova et al. 2017) based on lme4 (1.1-37; Bates et al. 2015) for the assays of Hb, TBARS, GST and for the fitness traits of GR_{mat} and $Size_{mat}$. For all the above traits, we performed a nested model comparison using the Likelihood Ratio Test to pick a model. We additionally used the performance package (v. 0.15.0; Lüdecke et al. 2021) as a confirmation of the comparison result. Model validation was performed using the performance package.

For Hb, TBARS and GST, the respective trait was set as the response variable and measurement *batch* was added as a random effect. The experimental block was not taken into consideration here as the randomly pooled replicates constituted of replicates from different blocks. For model comparisons, the following fixed terms were added one by one: *temperature* treatment, *clone*, *number of animals with eggs* in the sample, *number of animals with ephippia* in the sample and an *interaction term* between *temperature* and *clone*. The two terms of numbers of animals with eggs and ephippia respectively were added to account for potential effects the reproductive state of the animals might have had on the measured traits. The response variables for the oxygenated Hb peaks, TBARS and GST were log-transformed to better meet the assumptions of the model, although the results were similar with and without the log-transformation.

For the two fitness traits, GR_{mat} and $Size_{mat,}$ the random effect was *block* nested within *clone*, as we were interested to capture the possible random effect that a cohort of mothers could have had on the respective block of each clone. For the model comparison we likewise added the fixed terms one by one: *temperature*, *clone* and their *interaction*.

After the best model was picked for each trait, we performed a type III analysis of variance (ANOVA) using Satterthwaite's method (lmerTest package) and calculated the effect size omega^2 for each fixed effect with the package effectsize (v. 1.0.1; Ben-Shachar et al. 2020). Estimated marginal means and their 95% confidence intervals were estimated with the emmeans package and post-hoc comparisons with a Holm correction for multiple testing were performed by additionally inferring the 95% confidence intervals. Finally, Cohen's d and its 95% confidence intervals of the emmeans contrasts were estimated using the eff_size function from the emmeans package.

Mortality and $Time_{mat}$ data were analysed using the survival package (v. 3.8-3; Therneau 2024) to fit Cox proportional hazards models. *Block* was used as a frailty term (random effect term in Cox models), and *temperature* treatment and *clone* were used as fixed effects. Using a nested frailty term was not possible for this model. Both for Mortality and $Time_{mat}$, models were compared with a second model that included the *interaction* of *temperature* and *clone* as an additional effect, using the Likelihood Ratio test. The chosen model was tested for the assumption of proportional hazards by inspecting scaled Schoenfeld residual plots (Schoenfeld 1982). In the case of $Time_{mat}$, this assumption was violated both for *clone* and *temperature* and, therefore, the dataset was split into four time periods based on the residual plots, with the aim to have a constant hazard ratio within each period, as recommended by the respective vignette of the survival package (Therneau et al. 2024). The four time periods were: [0 - 14 days], [15 - 20 days], [21 - 25 days], and > 25 days. We then extended the Cox models by adding interactions of *clone* and *temperature* with a time-varying coefficient based on the stratified time periods and repeated the model comparison. Finally, estimated marginal means of the chosen models were calculated with the emmeans package (1.11.1; Lenth and Piaskowski 2025), and post-hoc tests were performed on them using the Holm correction for multiple testing (Holm 1979) and estimating 95% confidence intervals. For these estimations to be possible for the extended model, the frailty term of *block* was removed and the model refitted with *block* as a fixed term. For comparison, we performed the same analysis on the mortality and maturity data obtained from the animals of the physiological assays. Kaplan-Meier

survival curves and their 95% confidence intervals were drawn for all data using the survminer package (v. 0.5.0; Kassambara et al.) purely for visualisation, while the analysis was done as explained above.

All data and statistical analyses were performed in R (v. 4.3.0; R Core Team 2023) using Rstudio (v. 2025.09.0.387; Posit Team 2025). Plots were constructed using the ggplot2 package (v.3.5.2; Wickham 2016).

Results

Male production and mortality: During the entire experiment only one male was produced and subsequently removed. Mortality was likewise negligible and did not significantly reduce the number of experimental animals in either of the experimental modes. More specifically, survival did not fall below 80% for any clone or temperature and was therefore not further considered here.

Haemoglobin: Results for total haeme-containing proteins and the oxygenated Hb peaks were similar; therefore, we focus on the result for the relative oxygenated Hb peak at 576 nm. The selected model included *temperature* and *clone* as fixed factors. *Temperature* did not affect Hb levels for any of the clones, but *clone* had a significant effect with an effect size of 0.56 [95% CI: 0.35, 1.00], (Table 1a). Clone L11, the sole member of the modern genetic cluster included in the experiment, had significantly higher Hb compared with the other three clones in all treatments (Fig. 2a, see also Table S1a for model comparison and S2 for linear mixed model estimates and post-hoc test contrasts).

TBARS: In addition to *temperature* and *clone*, the selected model included *number of animals with eggs* (Table S1b). Although all three fixed effects had low p-values, the effect size was most substantial for *clone* (0.22 with 95% CI [0.02, 1.00]), following a phenotypic response pattern similar to Hb (Table 1b). Here again, TBARS concentration of clone L11 was significantly higher across all three temperatures compared with the other three clones (Fig. 2b and see Table S3 for extended results), indicating an elevated lipid peroxidation across temperatures in this clone. TBARS was

355 significantly higher in the 16°C treatment for all clones in comparison with the 14°C treatment with
356 an effect size of -0.91 with 95% CI [-1.73, -0.09]. In the 18°C treatment TBARS dropped closer to the
357 levels of 14°C in all clones, albeit without statistical significance.

358 *GST:* No model was selected from the Likelihood Ratio Test (Table S1c), as none explained the data
359 better than the null model containing only the random effect. To allow visual comparison with the
360 graph for the other traits, we fitted here the simplest model representing the experimental design,
361 namely with clone and temperature as fixed effects. As shown in Table 1c and Fig. 2c neither
362 temperature nor clone showed any effects on GST.

363 Table 1. Type III Analysis of Variance Table using Satterthwaite's method and Effect Size ω2 (partial) for linear
364 mixed models. Significant p-values ($p < 0.05$) and substantial effect sizes with 95% Confidence intervals (CI) not
365 including 0 are in bold. Ndf: Nominator degrees of freedom, Ddf: Denominator degrees of freedom

a. Relative oxygenated Haemoglobin peak at 576 nm

Chosen model: log($rPeak_{576}$) ~ 1 + Temperature + Clone + (1 | Batch)								
	Sum Sq.	Mean Sq.	Ndf	Ddf	F-value	p-value	Effect size ω^2 (partial)	95% CI
Temperature	0.11	0.06	2	37.03	1.65	0.205	0.03	[0.00, 1.00]
Clone	1.81	0.60	3	37.02	18.15	**2.08E-07**	**0.56**	**[0.35, 1.00]**

b. TBARS

Chosen model: log(TBARS) ~ 1 + Temperature + Clone + Nr. animals with eggs + (1 | Batch)								
	Sum Sq.	Mean Sq.	Ndf	Ddf	F-value	p-value	Effect size ω^2 (partial)	95% CI

Temperature	0.54	0.27	2	36.02	3.57	**0.038**	0.12	[0.00, 1.00]
Clone	1.09	0.36	3	36.25	4.79	**0.007**	**0.22**	**[0.02, 1.00]**
Nr. animals with eggs	0.32	0.32	1	37.49	4.16	**0.048**	0.07	[0.00, 1.00]

c. GST activity

Chosen model: Null; Fitted model: log(GST activity) ~ 1 + Temperature + Clone + (1 | Batch)								
	Sum Sq.	Mean Sq.	Ndf	Ddf	F-value	p-value	Effect size ω^2 (partial)	95% CI
Temperature	0.10	0.05	2	37.04	0.60	0.557	0	[0.00, 1.00]
Clone	0.25	0.08	3	37.04	1.02	0.394	0.001	[0.00, 1.00]

d. Growth rate to maturity (GR_{mat})

Chosen model: GR_{mat} ~ 1 + Temperature + Clone + Temperature:Clone + (1 | Clone:Block)								
	Sum Sq.	Mean Sq.	Ndf	Ddf	F-value	p-value	Effect size ω^2 (partial)	95% CI
Temperature	32194	16097.1	2	239.05	81.40	**< 2.2E-16**	**0.4**	**[0.32, 1.00]**
Clone	8209	2736.3	3	23.80	13.84	**1.99E-05**	**0.58**	**[0.32, 1.00]**
Temp:Clone	3004	500.6	6	240.42	2.53	**0.021**	0.04	[0.00, 1.00]

e. Size at maturity ($Size_{mat}$)

Chosen model: $Size_{mat}$ ~ 1 + Temperature + Clone + (1 | Clone:Block)								
	Sum Sq.	Mean Sq.	Num . df	Denom . df	F-value	p-value	Effect size ω^2 (partial)	95% CI
Temperature	106571	53286	2	232.56	3.85	**0.023**	0.02	[0.00, 1.00]
Clone	265785	88595	3	24.38	6.40	**0.002**	**0.36**	**[0.07, 1.00]**

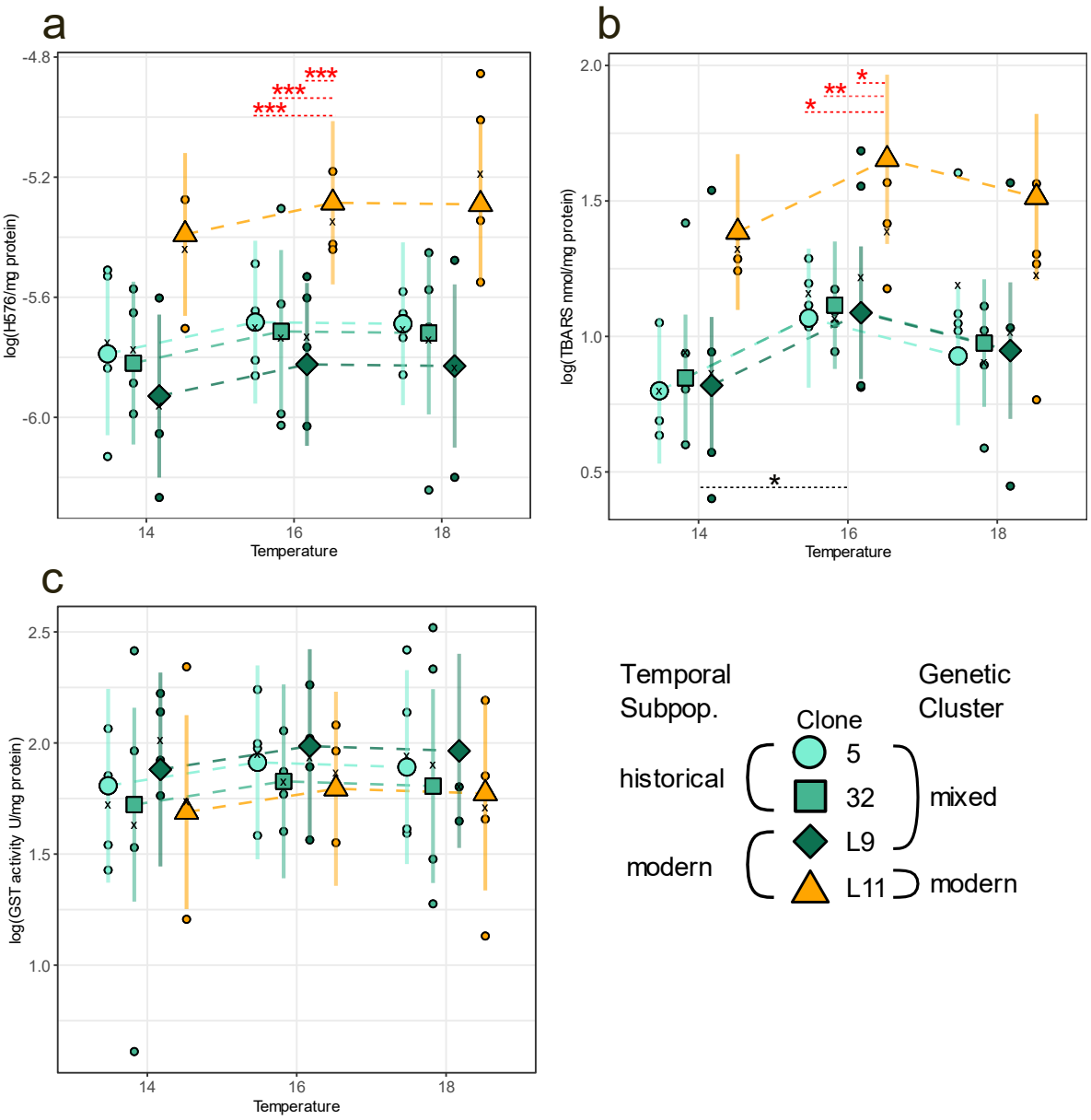

368

369 Figure 2. Physiological responses of four clones to elevated temperature. Panels show the measurement
370 results for the four clones for the relative oxygenated Haemoglobin peak at 576 nm per mg protein (a), TBARS
371 in nmol MDA/mg protein (b) and Glutathione-S-Transferase Activity in U/mg protein, where U equals substrate
372 conjugation min^{-1} (c). All responses were log-transformed. Big symbols represent estimated marginal means
373 per clone and temperature estimated from the chosen statistical model. Vertical bars represent their
374 confidence Intervals at a 95% threshold. Small points indicate raw measurements from the four pooled
375 replicates per clone and treatment, while "x" shows their arithmetic mean. Dashed lines connect the
376 estimated marginal means per clone. The legend explains the membership of each clone to temporal
377 subpopulation and genetic cluster. Black horizontal dashed bars with asterisks at the bottom of the plot

indicate overall statistically significant differences between temperature treatments from post-hoc contrasts with Holm correction. Red horizontal dashed bars with asterisks at the top of the plot indicate overall statistically significant differences between clones. Note that statistical differences between clones are averaged across temperatures as the models do not include an interaction term. Statistical significance of p-value is shown by asterisks thus: * < 0.05, ** < 0.01, *** < 0.001.

Growth rate to maturity: The chosen model for GR_{mat} included *temperature* and *clone* and their interaction (Table S1d). All three terms had a significant effect, although only the individual effect sizes of *clone* and *temperature* were substantial (> 0.1 and CIs did not include 0; Table 1d). This could be explained by the fact that temperature had a differing effect only for clone L11: While GR_{mat} of the mixed genetic cluster clones steadily increased in the tested temperature range, GR_{mat} for clone L11 only increased from 16°C to 18°C by a similar magnitude to the others (Fig. 3a, also see Table S4 for extended results), but not from 14°C to 16°C. At all temperatures, clone L11 had a lower GR_{mat} compared to the other three clones with statistical significance at 16°C and 18°C. Effect sizes were high (above 0.8) for all statistically significant post-hoc comparisons (see Table S4).

Size at maturity: The model chosen for this trait included only *temperature* and *clone* (Table S1e), but the overall effects were less strong than for GR_{mat} (Fig. 3b). Although both *temperature* and *clone* were significant, only *clone* had a substantial effect size (0.36 with 95% CI [0.07, 1.00]; Table 1e). $Size_{mat}$ decreased with elevated temperature for all clones (Fig. 3b and Table S5a). Animals were significantly smaller at 18°C compared with 14°C (Table S5b) and 18°C contrasts with both lower temperatures had substantial effect sizes (Table S5d). Clone L11 had a significantly larger $Size_{mat}$ across all temperatures compared with the other clones (Table S5).

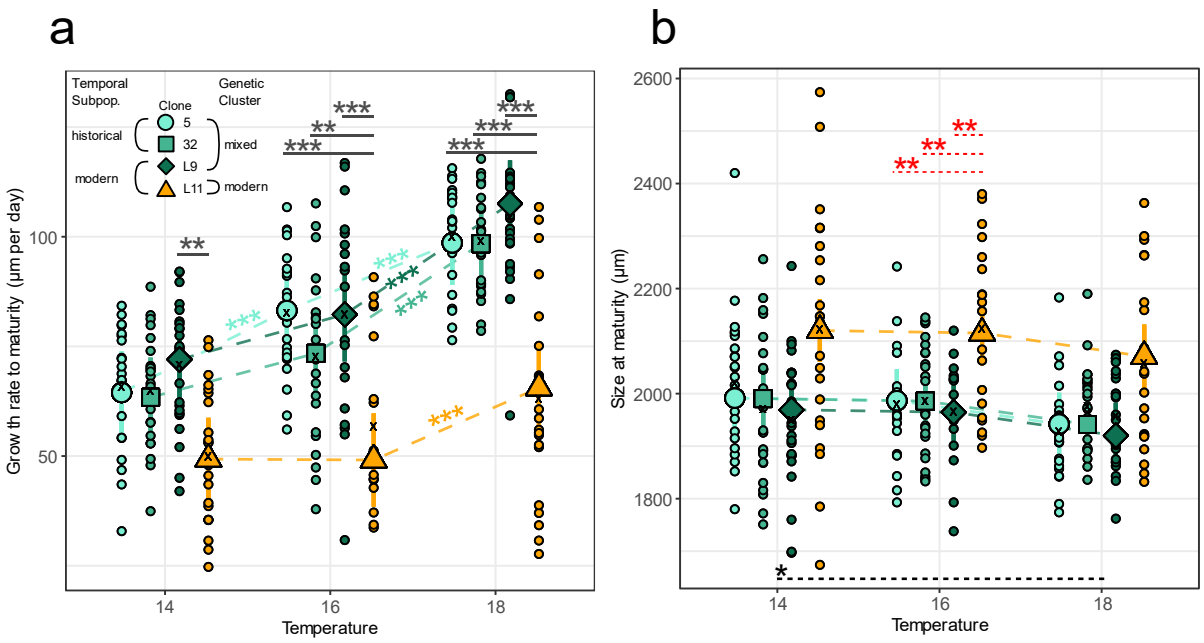

401

402 Figure 3. Life history trait responses of four clones to elevated temperature. Panels show the results for GR_{mat}
403 measured in µm per day (a) and $Size_{mat}$ in µm (b). Big symbols show the estimated marginal means per clone
404 and temperature estimated from the chosen statistical model and the vertical bars represent their confidence
405 Intervals at a 95% threshold. Small points indicate measurements from each individual per clone and
406 treatment, while "x" shows their arithmetic mean. Dashed lines connect the estimated marginal means per
407 clone. The legend explains the membership of each clone to temporal subpopulation and genetic cluster. Grey
408 horizontal bars with asterisks at the top of the plot in panel a indicate statistically significant differences
409 between clones within each temperature treatment (post-hoc contrasts, Holm correction). Coloured asterisks
410 on the dashed lines in panel a indicate statistical significance between successive temperatures within the
411 respective clone. The black dashed horizontal bar with asterisk at the bottom of the plot in panel b indicates
412 overall statistically significant difference between temperature treatments. Red horizontal dashed bars with
413 asterisks at the top of the plot indicate overall statistically significant differences between clones. Note that
414 statistical differences between clones in panel b are averaged across temperatures as the model does not
415 include an interaction term. Statistical significance of p-value is shown by asterisks thus: * < 0.05, ** < 0.01,
416 *** < 0.001.

417

Time to maturity: This trait, reflecting the number of days until the appearance of eggs in the brood chamber was significantly affected by *temperatur*e and *clone* (Table 2). Individuals at elevated temperatures mostly matured earlier, while clone L11 differed from the other three clones by overall slower maturation irrespective of temperature (Fig. 4). There was one outlier animal (from clone L9 at 16°C) that did not mature at all before dying at day 60, which was included in the analysis. *Temperature* affected $Time_{mat}$ significantly in the first 14 days (first time period) at both 16°C and 18°C, while in the second time period (from 15 to 20 days) individuals matured significantly earlier at 18°C (supported by the model estimates but not the post-hoc tests, see Table S6a, b). Clone L11 differed from all clones in the first 14 days, and from clones 5 and 32 in the second time period (Table S6c). There was no significant difference between clones or temperatures after day 20. The analysis of $Time_{mat}$ of individuals from the physiological assays produced the same pattern, confirming the above results (Fig. S1).

Table 2. Results from extended Cox model on $Time_{mat}$ from individuals of the fitness assays. Analysis of Deviance Table with Terms added sequentially (first to last, for details see Methods). Cox PH Model: Surv($Time_{mat}$, status) ~ Temp:strata(t) + Clone:strata(t) + frailty(Block). Significant p-values ($p < 0.05$) are in bold.

	Loglik.	Chisq	df	p-value
Null	-1311.3			
frailty(Block)	-1304.2	14.36	1	**1.51E-04**
Temp:strata(t)	-1241.9	124.59	8	**< 2.2e-16**
strata(t):Clone	-1199.7	84.29	14.77	**9.24E-12**

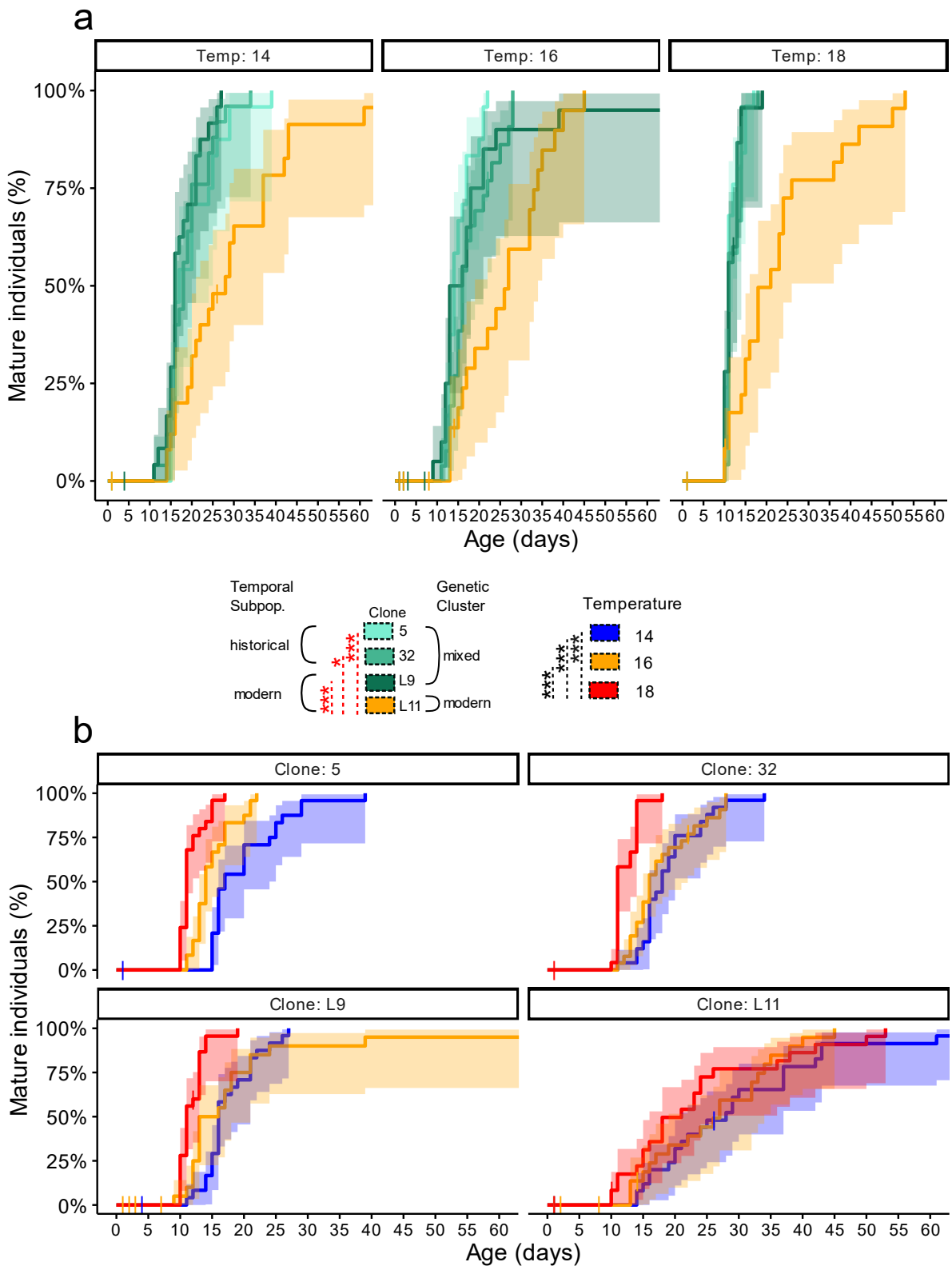

437

438 Figure 4. Kaplan-Meier curves for $Time_{mat}$ (here shown as age in days) of four clones across three

439 temperatures. Note that the real age at maturity could be plus 1-2 days, as the experiment started with up to

440 48h-old juveniles. The data originate from the fitness assays and are grouped by temperature in panel a) and

by clone in panel b). Ribbons around curves show the 95%. Confidence intervals and vertical lines are censored individuals. Red and black vertical dashed bars with asterisks on the legend indicate statistically significant differences from post-hoc contrasts with Holm correction from the Cox PH model between clones and temperatures respectively, only for the first time period [0, 14 days]. Statistical significance of p-value is shown by asterisks thus: * < 0.05, ** < 0.01, *** < 0.001.

Discussion

In this study we compared physiological and life history responses of four arctic *Daphnia pulicaria* clones from two temporal subpopulations from Braya Sø in South-West Greenland. We found that the responses of all three clones from the mixed genetic cluster where more similar to each other than to clone L11 from the modern cluster. This modern clone differed from the other three clones as expected by higher haemoglobin level, higher values of lipid peroxidation, slower growth rates, and later maturity, all indicating higher stress levels. Contrary to our expectations, the physiological measurements did not clearly show an increased level of stress with higher temperature, while one of the markers, GST activity, did not show a pattern between the tested temperatures or differences between clones at all. The obtained results are discussed in detail below.

Genetic cluster membership determines physiological and life history responses

The genetic cluster membership was the only determinant for the clones' response patterns, despite a significant difference in thermal tolerance between temporal subpopulations in our previous work (Karapli-Petritsopoulou et al. 2025b). One possible explanation for this discrepancy is that we previously characterised thermal tolerance using an acute measurement, i.e. time to immobilisation at 34°C, while here we were measuring more chronic physiological responses to milder thermal stress, essentially assessing different traits. Clone L11 associated with the modern genetic cluster differed significantly from the three mixed cluster clones in almost all traits. Responses of the latter were mostly identical for the traits measured, despite the different temporal origin of the clones.

This could be expected also by the extremely low genetic distances between the clones of the same genetic cluster (Karapli-Petritsopoulou et al. 2025b), although identical genomes do not necessarily preclude phenotypic divergence if there are different epigenetic marks (Feiner et al. 2022; Vogt 2022).

The consistently higher haemoglobin level and lipid peroxidation of clone L11 coupled with slower growth rate and later maturity, suggest that this clone is under more stress. While higher biomarker values could also be coupled with higher tolerance for this stress, and therefore may not indicate a fitness disadvantage (Coggins et al. 2017), our previous work has shown a lower thermal tolerance of clone L11 in comparison to the other three (Karapli-Petritsopoulou et al. 2025b). The temperature of 14°C used as control here can already be considered high for this ecosystem, as it represents the surface temperature typically reached in the warmest summer months. It is possible that the *Daphnia* may not experience this high temperature by seeking refuge in the colder lower depths, however Braya Sø has a permanent anoxic zone that would cause additional hypoxic stress (Karapli-Petritsopoulou et al. 2025b). In principle, thermal and hypoxic stress pose similar physiological challenges, as they are both bound to oxygen capacity (Pörtner 2010). It is therefore possible that clone L11, and therefore likely all genetically highly similar representatives of the modern genetic cluster detected only in 2022 are less fit under future temperature scenarios, raising the question whether these genotypes will be able to persist.

Elevated temperatures did not result in higher thermal stress

Contradicting our expectations, thermal stress measured by the physiological biomarkers did not have a clear pattern of increase with higher temperature within the tested range. Life history traits, however, were more responsive to the tested temperatures.

Haemoglobin levels were not elevated at 16°C or 18°C in comparison to 14°C in any of the clones. It could be that the tested temperature range was not high enough to induce any excess thermal stress surpassing the capabilities of the baseline haemoglobin level. It is unlikely that a 4°C range

was too narrow: In the temperate species *Daphnia pulex* individuals both acclimated and acutely exposed to 24°C had higher Hb concentration compared with individuals acclimated to 20°C (Gerke et al. 2011; Zeis et al. 2013). While increasing haemoglobin content with warmer temperatures in *Daphnia* is one of the possible responses, another known response is an alteration of the oxygen binding affinity of Hb mainly through differential subunit composition of the molecule, increasing its efficiency (Zeis 2020). Such a change in the subunit composition could be an alternative strategy to an increase in Hb level in the tested clones, but cannot currently be determined from our data. Conversely, it is possible that the Arctic *Daphnia pulicaria* lack Hb production plasticity as Hb plasticity is known to be dependent upon clone (Pinkhaus et al. 2007; Yampolsky et al. 2014; Cuenca Cambronero et al. 2018) and species (Sell 1998; Zeis 2020). Interestingly, Yampolsky et al. (2014) found that *Daphnia magna* clones originating from colder environments had a significant trend of lower plasticity in Hb production compared with clones from warmer environments.

Lipid peroxidation was significantly higher for all clones at 16°C compared with 14°C, while it dropped again at 18°C. Lipid peroxidation can be a useful marker for assessing oxidative damage, but its level is affected both by antioxidant capacity and lipid composition that cannot be disentangled from our data. The amount of polyunsaturated fatty acids (PUFAs) in the lipid composition of the membranes depends on temperature as well as on the genotype (Martin-Creuzburg et al. 2019; Zeis et al. 2019; Werner et al. 2021). As PUFAs are primary targets of lipid peroxidation, the more PUFAs present in cell membranes, the higher lipid peroxidation is expected (Ayala et al. 2014; Zeis et al. 2019). *Daphnia* have a higher accumulation of PUFAs at lower temperatures, as they are important for the fluidity of biomembranes (Zeis et al. 2019). Assuming that excess oxidative damage occurs above 14°C, the lipid composition might have remained unchanged at 16 °C, while at 18 °C, the temperature may have been high enough to initiate membrane restructuring with reduced PUFAs (Crockett 2008). Another possibility is that at 18°C, antioxidant defence systems (other than the GST enzyme that we measured) were activated that reduced oxidative damage and, consequently, lipid peroxidation.

Growth rate to maturity was more sensitive to temperature and was higher at elevated temperatures for all clones as expected, even though clone L11 had a significantly higher growth rate only at 18°C, as discussed above. Higher GR_{mat} as well as shorter $Time_{mat}$ is consistent with higher metabolic and development rates occurring at elevated temperatures in ectotherms including *Daphnia* (Gillooly et al. 2001; Forster et al. 2011; Fossen et al. 2018; Im et al. 2019). However, elevated oxidative stress can result in the allocation of a limited amount of energy to growth and reproduction, a trade-off that has been observed in other *Daphnia* species (Smith et al. 2016; Im et al. 2020b) and may explain the lower growth rate and later reproduction of clone L11. Consequently, the significantly higher $Size_{mat}$ of clone L11 can be expected from its significantly later reproduction. $Size_{mat}$ did not change across temperatures for any of the clones, suggesting that this trait might not be as sensitive to this low temperature range as the other measured traits. A lower plasticity of $Size_{mat}$ compared with $Time_{mat}$ is also supported by thermal reaction norms reported for *Daphnia magna* in other studies (Fossen et al. 2018; Hoefnagel et al. 2018).

The negligible differences in thermal stress we observed between the tested temperatures may also be linked to the presence of an anoxic zone in this population's habitat (Karapli-Petritsopoulou et al. 2025b): an elevated hypoxia tolerance of the *Daphnia* of Braya Sø has been suggested by previous results (Karapli-Petritsopoulou et al. 2025a; b), linked to the migration of *Daphnia* to the lower, anoxic depths for the purpose of exploiting additional food resources (Massana et al. 1994; Sell 1998) historically present in the oxycline of this meromictic oligotrophic lake (Dane et al. 2020). Because of the central role of oxygen limitation in thermal tolerance (Paul et al. 2004; Seidl et al. 2005; Pörtner 2010), an elevated tolerance to hypoxia could be protective against the thermal stress caused within the temperature range tested here.

GST activity did not differ

We did not find any differences or trends between clones and temperatures for GST activity. It is possible that the experimental exposure temperatures did not produce sufficient oxidative stress to

trigger the further activation of antioxidant defence systems compared to our control temperature. This is supported by the lack of elevated haemoglobin and low lipid peroxidation at 18°C, if the latter was a result of a membrane reconstruction, as discussed above. Alternatively, there may have been an activation of other antioxidant enzymes as each enzyme responds differently according to the stressor or toxicant (Barata et al. 2005b). Although the glutathione redox system is activated by exposure to a rise in temperature in *Daphnia* (Becker et al. 2011), studies comparing different enzyme response to thermal stress demonstrated no significant increase in GST activity in contrast to glutathione peroxidase and catalase (Im et al. 2019; Hoffschröer et al. 2024).

Conclusion

Our study addresses the complex interplay between thermal stress under potential future climate scenarios and life history traits as well as oxidative stress responses of an Arctic OP *Daphnia pulicaria* from two different time periods. Our results demonstrate strong similarity of all measured traits among clones of the same genetic cluster, while there was no effect of the time period of their origin, indicative of a lack of micro-evolutionary change. The temperatures tested did not induce plasticity in the physiological markers in any of the clones, suggesting that these *Daphnia* are protected from thermal stress at the tested temperature range, but also raising the question whether additional markers could offer further insights into physiological changes across the three temperatures. Finally, the clone representing the modern genetic cluster that was detected only in 2022 showed overall higher stress levels and lower fitness. A more in-depth survey of this population is needed to assess its overall survival capacity and consequences to the lake ecosystem.

Our study included markers for different physiological processes. Although we were only able to include one clone from the modern genetic cluster, our data suggest a high likelihood that clones from the same genetic cluster will have very similar responses. A deeper understanding of physiological responses to thermal stress in these clones would require direct measurements of oxidative stress (ROS) as well as enzymes of other antioxidant defence systems like catalase and

superoxide dismutase. In addition, a wider range of both lower and higher temperatures would allow the construction of thermal performance curves (TPCs) (Wang et al. 2023) that could help to determine the optimum temperatures of these clones. As environmental change generates multiple stressors that influence organismal responses (Altshuler et al. 2011), future research in this system should include various interacting stressors while incorporating variable rather than constant temperature changes in the design to achieve greater ecological relevance (Chen and Stillman 2012).

Acknowledgements

We are grateful to the Government of Greenland for granting Prior Informed Consent for utilization of Greenland genetic resources (non-exclusive licence no. G22-076) that permits collection and basic research on genetic resources. This work formed part of the doctoral thesis of Athina Karapli-Petritsopoulou (Freie Universität Berlin, 2026).

Competing interests

The authors have no competing interests to declare.

Author contributions

Conceptualization: AKP, DB, DF; Methodology: AKP, DB, DF; Formal analysis: AKP; Investigation: AKP, DF; Resources: DB, DF; Writing – original draft preparation: AKP; Writing – review and editing: AKP, DB, DF; Visualisation: AKP; Supervision: DB, DF; Project administration: DF; Funding acquisition: DF

Funding

This research was funded by the Deutsche Forschungsgemeinschaft (DFG, German Research Foundation) – Project number 461099895.

Data availability

The data and code that support the findings of this study will be openly available in Zenodo upon publication.

References

Altshuler, I., B. Demiri, S. Xu, A. Constantin, N. D. Yan, and M. E. Cristescu. 2011. An Integrated Multi-Disciplinary Approach for Studying Multiple Stressors in Freshwater Ecosystems: *Daphnia* as a Model Organism. Integr Comp Biol **51**: 623–633. doi:10.1093/icb/icr103

Anderson, N. J. and others. 2017. The Arctic in the Twenty-First Century: Changing Biogeochemical Linkages across a Paraglacial Landscape of Greenland. BioScience **67**: 118–133. doi:10.1093/biosci/biw158

Ayala, A., M. F. Muñoz, and S. Argüelles. 2014. Lipid Peroxidation: Production, Metabolism, and Signaling Mechanisms of Malondialdehyde and 4-Hydroxy-2-Nonenal. Oxidative Medicine and Cellular Longevity **2014**: 360438. doi:10.1155/2014/360438

Bae, E., P. Samanta, J. Yoo, and J. Jung. 2016. Effects of multigenerational exposure to elevated temperature on reproduction, oxidative stress, and Cu toxicity in *Daphnia magna*. Ecotoxicology and Environmental Safety **132**: 366–371. doi:10.1016/j.ecoenv.2016.06.034

Barata, C., J. Carlos Navarro, I. Varo, M. Carmen Riva, S. Arun, and C. Porte. 2005a. Changes in antioxidant enzyme activities, fatty acid composition and lipid peroxidation in *Daphnia magna* during the aging process. Comparative Biochemistry and Physiology Part B: Biochemistry and Molecular Biology **140**: 81–90. doi:10.1016/j.cbpc.2004.09.025

614 Barata, C., I. Varo, J. C. Navarro, S. Arun, and C. Porte. 2005b. Antioxidant enzyme activities and lipid
615 peroxidation in the freshwater cladoceran *Daphnia magna* exposed to redox cycling
616 compounds. Comparative Biochemistry and Physiology Part C: Toxicology & Pharmacology
617 **140**: 175–186. doi:10.1016/j.cca.2005.01.013
618 Bates, D., M. Mächler, B. Bolker, and S. Walker. 2015. Fitting Linear Mixed-Effects Models Using
619 lme4. Journal of Statistical Software **67**: 1–48. doi:10.18637/jss.v067.i01
620 Becker, D. and others. 2018. The transcriptomic and proteomic responses of *Daphnia pulex* to
621 changes in temperature and food supply comprise environment-specific and clone-specific
622 elements. BMC Genomics **19**: 1–30. doi:10.1186/s12864-018-4742-6
623 Becker, D., B. F. Brinkmann, B. Zeis, and R. J. Paul. 2011. Acute changes in temperature or oxygen
624 availability induce ROS fluctuations in *Daphnia magna* linked with fluctuations of reduced
625 and oxidized glutathione, catalase activity and gene (haemoglobin) expression. Biology of
626 the Cell **103**: 351–363. doi:10.1042/BC20100145
627 Bennett, S., C. M. Duarte, N. Marbà, and T. Wernberg. 2019. Integrating within-species variation in
628 thermal physiology into climate change ecology. Philosophical Transactions of the Royal
629 Society B: Biological Sciences **374**: 20180550. doi:10.1098/rstb.2018.0550
630 Ben-Shachar, M. S., D. Lüdecke, and D. Makowski. 2020. effectsize: Estimation of Effect Size Indices
631 and Standardized Parameters. Journal of Open Source Software **5**: 2815.
632 doi:10.21105/joss.02815
633 Borgeraas, J., and D. O. Hessen. 2000. UV-B induced mortality and antioxidant enzyme activities in
634 *Daphnia magna* at different oxygen concentrations and temperatures. J Plankton Res **22**:
635 1167–1183. doi:10.1093/plankt/22.6.1167
636 Bradford, M. M. 1976. A rapid and sensitive method for the quantitation of microgram quantities of
637 protein utilizing the principle of protein-dye binding. Analytical Biochemistry **72**: 248–254.
638 doi:10.1016/0003-2697(76)90527-3

639 Burton, T., B. Zeis, and S. Einum. 2018. Automated measurement of upper thermal limits in small
640 aquatic animals. 1-5. doi:10.1242/jeb.182386
641 Catullo, R. A., J. Llewelyn, B. L. Phillips, and C. C. Moritz. 2019. The Potential for Rapid Evolution
642 under Anthropogenic Climate Change. Current Biology **29**: R996–R1007.
643 doi:10.1016/j.cub.2019.08.028
644 Chen, X., and J. H. Stillman. 2012. Multigenerational analysis of temperature and salinity variability
645 affects on metabolic rate, generation time, and acute thermal and salinity tolerance in
646 *Daphnia pulex*. Journal of Thermal Biology **37**: 185–194. doi:10.1016/j.jtherbio.2011.12.010
647 Chown, S. L., A. A. Hoffmann, T. N. Kristensen, M. J. A. Jr, N. C. Stenseth, and C. Pertoldi. 2010.
648 Adapting to climate change: a perspective from evolutionary physiology. Climate Research
649 **43**: 3–15. doi:10.3354/cr00879
650 Coggins, B. L., J. W. Collins, K. J. Holbrook, and L. Y. Yampolsky. 2017. Antioxidant capacity, lipid
651 peroxidation, and lipid composition changes during long-term and short-term thermal
652 acclimation in *Daphnia*. J Comp Physiol B **187**: 1091–1106. doi:10.1007/s00360-017-1090-9
653 Colbourne, J. K., T. J. Crease, L. J. Weider, P. D. N. Hebert, F. Duferesne, and A. Hobaek. 1998.
654 Phylogenetics and evolution of a circumarctic species complex (Cladocera: *Daphnia pulex*).
655 Biological Journal of the Linnean Society **65**: 347–365. doi:10.1111/J.1095-
656 8312.1998.TB01146.X
657 Crockett, E. L. 2008. The cold but not hard fats in ectotherms: consequences of lipid restructuring on
658 susceptibility of biological membranes to peroxidation, a review. J Comp Physiol B **178**: 795–
659 809. doi:10.1007/s00360-008-0275-7
660 Cuenca Cambronero, M., B. Zeis, and L. Orsini. 2018. Haemoglobin-mediated response to hyper-
661 thermal stress in the keystone species *Daphnia magna*. Evolutionary Applications **11**: 112–
662 120. doi:10.1111/eva.12561

663 Dane, M., N. J. Anderson, C. L. Osburn, J. K. Colbourne, and D. Frisch. 2020. Centennial clonal
664 stability of asexual *Daphnia* in Greenland lakes despite climate variability. Ecology and
665 Evolution **10**: 14178–14188. doi:10.1002/ece3.7012
666 Dufresne, F., and P. D. N. Hebert. 1997. Pleistocene glaciations and polyphyletic origins of polyploidy
667 in an arctic cladoceran. Proceedings of the Royal Society of London. Series B: Biological
668 Sciences **264**: 201–206. doi:10.1098/rspb.1997.0028
669 Ebert, D. 2022. *Daphnia* as a versatile model system in ecology and evolution. EvoDevo **13**: 16.
670 doi:10.1186/s13227-022-00199-0
671 Feiner, N. and others. 2022. Environmentally induced DNA methylation is inherited across
672 generations in an aquatic keystone species. iScience **25**: 104303.
673 doi:10.1016/j.isci.2022.104303
674 Forster, J., A. G. Hirst, and G. Woodward. 2011. Growth and Development Rates Have Different
675 Thermal Responses. The American Naturalist **178**: 668–678. doi:10.1086/662174
676 Fossen, E. I. F., C. Pélabon, and S. Einum. 2018. An empirical test for a zone of canalization in thermal
677 reaction norms. Journal of Evolutionary Biology **31**: 936–943. doi:10.1111/jeb.13287
678 Frisch, D., P. K. Morton, P. R. Chowdhury, B. W. Culver, J. K. Colbourne, L. J. Weider, and P. D.
679 Jeyasingh. 2014. A millennial-scale chronicle of evolutionary responses to cultural
680 eutrophication in *Daphnia*. Ecology Letters **17**: 360–368. doi:10.1111/ele.12237
681 Geerts, A. N. and others. 2015. Rapid evolution of thermal tolerance in the water flea *Daphnia*.
682 Nature Climate Change **5**: 665–668. doi:10.1038/nclimate2628
683 Gerke, P., C. Börding, B. Zeis, and R. J. Paul. 2011. Adaptive haemoglobin gene control in *Daphnia*
684 *pulex* at different oxygen and temperature conditions. Comparative Biochemistry and
685 Physiology - A Molecular and Integrative Physiology **159**: 56–65.
686 doi:10.1016/j.cbpa.2011.01.017
687 Gillooly, J. F., J. H. Brown, G. B. West, V. M. Savage, and E. L. Charnov. 2001. Effects of Size and
688 Temperature on Metabolic Rate. Science **293**: 2248–2251. doi:10.1126/science.1061967

689 Hairston, N. G. and others. 1999. Rapid evolution revealed by dormant eggs. Nature **401**: 446–446.
690 doi:10.1038/46731
691 Hoefnagel, K. N., E. H. J. (Lisenka) de Vries, E. Jongejans, and W. C. E. P. Verberk. 2018. The
692 temperature-size rule in *Daphnia magna* across different genetic lines and ontogenetic
693 stages: Multiple patterns and mechanisms. Ecol Evol **8**: 3828–3841. doi:10.1002/ece3.3933
694 Hoffschröer, N., C. Laspoumaderes, B. Zeis, and N. Tremblay. 2024. Mitochondrial metabolism and
695 respiration adjustments following temperature acclimation in *Daphnia magna*. Journal of
696 Thermal Biology **119**: 103761. doi:10.1016/j.jtherbio.2023.103761
697 Holm, S. 1979. A Simple Sequentially Rejective Multiple Test Procedure. Scandinavian Journal of
698 Statistics **6**: 65–70. https://www.jstor.org/stable/4615733
699 Im, H., J. Na, and J. Jung. 2020a. Multigenerational plasticity of *Daphnia magna* under thermal stress
700 across ten generations. Ecotoxicology and Environmental Safety **194**: 110400.
701 doi:10.1016/j.ecoenv.2020.110400
702 Im, H., J. Na, and J. Jung. 2020b. The effect of food availability on thermal stress in *Daphnia magna*:
703 trade-offs among oxidative stress, somatic growth, and reproduction. Aquat Ecol **54**: 1201–
704 1210. doi:10.1007/s10452-020-09804-7
705 Im, H., P. Samanta, J. Na, and J. Jung. 2019. Time-Dependent Responses of Oxidative Stress, Growth,
706 and Reproduction of *Daphnia magna* Under Thermal Stress. Bull Environ Contam Toxicol
707 **102**: 817–821. doi:10.1007/s00128-019-02613-1
708 Innes, D. J., and F. Dufresne. 2020. Parthenogenesis, p. 0. *In* R. Cothran and M. Thiel [eds.],
709 Reproductive Biology: The Natural History of the Crustacea, Volume 6. Oxford University
710 Press.
711 Karapli-Petritsopoulou, A., J. J. Heckelmann, N. J. Anderson, S. Franzenburg, and D. Frisch. 2025a.
712 Phenotypic Divergence Associated With Genomic Changes Suggests Physiological Adaptation
713 in Obligate Asexuals. Freshwater Biology **70**: e70111. doi:10.1111/fwb.70111

Karapli-Petritsopoulou, A., J. J. Heckelmann, D. Becker, N. J. Anderson, and D. Frisch. 2025b. Altered Phenotypic Responses of Asexual Arctic *Daphnia* After 10 Years of Rapid Climate Change. Global Change Biology **31**: e70119. doi:10.1111/gcb.70119

Kassambara A, Kosinski M, and Biecek P. survminer: Drawing Survival Curves using "ggplot2." R package version 0.5.1, https://CRAN.R-project.org/package=survminer

Khan, Q., and M. Khan. 2008. Effect of temperature on waterflea *Daphnia magna* (Crustacea:Cladocera). Nat Prec 1–1. doi:10.1038/npre.2008.1909.1

Kielland, Ø. N., C. Bech, and S. Einum. 2019. Warm and out of breath: Thermal phenotypic plasticity in oxygen supply. Functional Ecology **33**: 2142–2149. doi:10.1111/1365-2435.13449

Kuznetsova, A., P. B. Brockhoff, and R. H. B. Christensen. 2017. lmerTest package: Tests in linear mixed effects models. Journal of Statistical Software **82**: 1–26. doi:10.18637/jss.v082.i13

Lamkemeyer, T., B. Zeis, and R. J. Paul. 2003. Temperature acclimation influences temperature-related behaviour as well as oxygen-transport physiology and biochemistry in the water flea *Daphnia magna*. Can. J. Zool. **81**: 237–249. doi:10.1139/z03-001

Lampert, W. 2011. *Daphnia*: Development of a Model Organism in Ecology and Evolution. Excellence in Ecology. 21.

Lenth R and Piaskowski J. 2025. emmeans: Estimated Marginal Means, aka Least-Squares Means. R package version 1.11.1, https://CRAN.R-project.org/package=emmeans

Lüdecke, D., M. S. Ben-Shachar, I. Patil, P. Waggoner, and D. Makowski. 2021. performance: An R Package for Assessment, Comparison and Testing of Statistical Models. Journal of Open Source Software **6**: 3139. doi:10.21105/joss.03139

Lushchak, V. I. 2011. Environmentally induced oxidative stress in aquatic animals. Aquatic Toxicology **101**: 13–30. doi:10.1016/j.aquatox.2010.10.006

Martin-Creuzburg, D., B. L. Coggins, D. Ebert, and L. Y. Yampolsky. 2019. Rearing Temperature and Fatty Acid Supplementation Jointly Affect Lipid Fluorescence Polarization and Heat Tolerance in *Daphnia*. Physiological and Biochemical Zoology **92**: 408–418. doi:10.1086/704365

740 Massana, R., J. M. Gasol, K. Jürgens, and C. Pedròs-Aliò. 1994. Impact of *Daphnia pulex* on a
741 metalimnetic microbial community. Journal of Plankton Research **16**: 1379–1399.
742 doi:10.1093/plankt/16.10.1379
743 Miner, B. E., L. De Meester, M. E. Pfrender, W. Lampert, and N. G. Hairston. 2012. Linking genes to
744 communities and ecosystems: *Daphnia* as an ecogenomic model. Proceedings of the Royal
745 Society B: Biological Sciences **279**: 1873–1882. doi:10.1098/rspb.2011.2404
746 Nauen, R., and N. Stumpf. 2002. Fluorometric Microplate Assay to Measure Glutathione *S*-
747 Transferase Activity in Insects and Mites Using Monochlorobimane. Analytical Biochemistry
748 **303**: 194–198. doi:10.1006/abio.2002.5578
749 Oexle, S., M. Jansen, K. Pauwels, R. Sommaruga, L. De Meester, and R. Stoks. 2016. Rapid evolution
750 of antioxidant defence in a natural population of *Daphnia magna*. j. evol. Biol. **29**: 1328–
751 1337. doi:10.1111/jeb.12873
752 Ohkawa, H., N. Ohishi, and K. Yagi. 1979. Assay for lipid peroxides in animal tissues by thiobarbituric
753 acid reaction. Analytical Biochemistry **95**: 351–358. doi:10.1016/0003-2697(79)90738-3
754 Pamplona, R., and D. Costantini. 2011. Molecular and structural antioxidant defenses against
755 oxidative stress in animals. American Journal of Physiology-Regulatory, Integrative and
756 Comparative Physiology **301**: R843–R863. doi:10.1152/ajpregu.00034.2011
757 Paul, R. J., M. Colmorgen, S. Hüller, F. Tyroller, and D. Zinkler. 1997. Circulation and respiratory
758 control in millimetre-sized animals (*Daphnia magna*, *Folsomia candida*) studied by optical
759 methods. J Comp Physiol B **167**: 399–408. doi:10.1007/s003600050089
760 Paul, R. J., T. Lamkemeyer, J. Maurer, O. Pinkhaus, R. Pirow, M. Seidl, and B. Zeis. 2004. Thermal
761 acclimation in the microcrustacean *Daphnia*: a survey of behavioural, physiological and
762 biochemical mechanisms. Journal of Thermal Biology **29**: 655–662.
763 doi:10.1016/j.jtherbio.2004.08.035
764 Pecl, I., P. U. Blier, and F. Dufresne. 2025. Fatty acid profiles and tolerance to temperature extremes
765 in *Daphnia pulex*. J Exp Biol **228**: JEB249589. doi:10.1242/jeb.249589

766 Phosphate-buffered saline (PBS). 2006. Cold Spring Harb Protoc **2006**: pdb.rec8247.
767 doi:10.1101/pdb.rec8247
768 Pinkhaus, O. and others. 2007. Temporal environmental change, clonal physiology and the genetic
769 structure of a *Daphnia* assemblage (*D. galeata–hyalina* hybrid species complex). Freshwater
770 Biology **52**: 1537–1554. doi:10.1111/j.1365-2427.2007.01786.x
771 Pörtner, H. 2001. Climate change and temperature-dependent biogeography: oxygen limitation of
772 thermal tolerance in animals. Naturwissenschaften **88**: 137–146.
773 doi:10.1007/s001140100216
774 Pörtner, H. O. 2002. Climate variations and the physiological basis of temperature dependent
775 biogeography: systemic to molecular hierarchy of thermal tolerance in animals. Comparative
776 Biochemistry and Physiology Part A: Molecular & Integrative Physiology **132**: 739–761.
777 doi:10.1016/S1095-6433(02)00045-4
778 Pörtner, H.-O. 2010. Oxygen- and capacity-limitation of thermal tolerance: a matrix for integrating
779 climate-related stressor effects in marine ecosystems. J Exp Biol **213**: 881–893.
780 doi:10.1242/jeb.037523
781 Posit Team. 2025. RStudio: Integrated Development Environment for R. Posit Software, PBC,Boston,
782 MA. URL http://www.posit.co/
783 Prowse, T. D., F. J. Wrona, J. D. Reist, J. E. Hobbie, L. M. J. Lévesque, and W. F. Vincent. 2006. General
784 Features of the Arctic Relevant to Climate Change in Freshwater Ecosystems. ambi **35**: 330–
785 338. doi:10.1579/0044-7447(2006)35%5B330:GFOTAR%5D2.0.CO;2
786 Przytulska, A., M. Bartosiewicz, M. Rautio, F. Dufresne, and W. F. Vincent. 2015. Climate Effects on
787 High Latitude *Daphnia* via Food Quality and Thresholds. PLOS ONE **10**: e0126231.
788 doi:10.1371/journal.pone.0126231
789 R Core Team. 2023. R: a language and environment for statistical computing. R Foundation for
790 Statistical Computing, Vienna, Austria. <https://www.R-project.org/>

791 Samanta, P., H. Im, T. Shim, J. Na, and J. Jung. 2020. Linking multiple biomarker responses in *Daphnia*
792 *magna* under thermal stress. Environmental Pollution **263**: 114432.
793 doi:10.1016/j.envpol.2020.114432
794 Saros, J. E. and others. 2025. Abrupt transformation of west Greenland lakes following compound
795 climate extremes associated with atmospheric rivers. Proceedings of the National Academy
796 of Sciences **122**: e2413855122. doi:10.1073/pnas.2413855122
797 Schoenfeld, D. 1982. Partial residuals for the proportional hazards regression model. Biometrika **69**:
798 239–241. doi:10.1093/biomet/69.1.239
799 Schwerin, S., B. Zeis, T. Lamkemeyer, R. J. Paul, M. Koch, J. Madlung, C. Fladerer, and R. Pirow. 2009.
800 Acclimatory responses of the *Daphnia pulex* proteome to environmental changes. II. Chronic
801 exposure to different temperatures (10 and 20°C) mainly affects protein metabolism. BMC
802 Physiology **9**. doi:10.1186/1472-6793-9-8
803 Seidl, M. D., R. Pirow, and R. J. Paul. 2005. Acclimation of the microcrustacean *Daphnia magna* to
804 warm temperatures is dependent on haemoglobin expression. Journal of Thermal Biology
805 **30**: 532–544. doi:10.1016/j.jtherbio.2005.06.004
806 Sell, A. F. 1998. Adaptation to oxygen deficiency: Contrasting patterns of haemoglobin synthesis in
807 two coexisting *Daphnia* species. Comparative Biochemistry and Physiology Part A: Molecular
808 & Integrative Physiology **120**: 119–125. doi:10.1016/S1095-6433(98)10019-3
809 Smith, S. M., R. G. Nager, and D. Costantini. 2016. Meta-analysis indicates that oxidative stress is
810 both a constraint on and a cost of growth. Ecology and Evolution **6**: 2833–2842.
811 doi:10.1002/ece3.2080
812 Sugano, H., and T. Hoshi. 1971. Purification and properties of blood hemoglobin from the fresh-
813 water cladocera, *Moina macrocopa* and *Daphnia magna*. Biochimica et Biophysica Acta
814 (BBA) - Protein Structure **229**: 349–358. doi:10.1016/0005-2795(71)90194-2
815 Therneau T. 2024. A Package for Survival Analysis in R. R package version 3.8-3, https://CRAN.R-
816 project.org/package=survival

817 Therneau, T., C. Crowson, and E. Atkinson. 2024. Using Time Dependent Covariates and Time
818 Dependent Coefficients in the Cox Model. *Survival Vignettes* https://cran.r-
819 project.org/web/packages/survival/vignettes/timedep.pdf
820 Vogt, G. 2022. Studying phenotypic variation and DNA methylation across development, ecology and
821 evolution in the clonal marbled crayfish: a paradigm for investigating epigenotype-
822 phenotype relationships in macro-invertebrates. Sci Nat **109**: 16. doi:10.1007/s00114-021-
823 01782-6
824 Wang, Y.-J., N. Tüzün, L. De Meester, H. Feuchtmayr, A. Sentis, and R. Stoks. 2023. Rapid evolution of
825 unimodal but not of linear thermal performance curves in *Daphnia magna*. Proc. R. Soc. B.
826 **290**: 20222289. doi:10.1098/rspb.2022.2289
827 Weider, L. J., and P. D. N. Hebert. 1987. Ecological and Physiological Differentiation Among Low-Artic
828 Clones of *Daphnia pulex*. Ecology **68**: 188–198. doi:10.2307/1938819
829 Weider, L. J., A. Hobæk, J. K. Colbourne, T. J. Crease, F. Dufresne, and P. D. N. Hebert. 1999. Holarctic
830 Phylogeography of an asexual species complex I. Mitochondrial DNA variation in arctic
831 *Daphnia*. Evolution **53**: 777–792. doi:10.1111/j.1558-5646.1999.tb05372.x
832 Weider, L. J., P. D. Jeyasingh, and D. Frisch. 2018. Evolutionary aspects of resurrection ecology:
833 Progress, scope, and applications—An overview. Evolutionary Applications **11**: 3–10.
834 doi:10.1111/eva.12563
835 Werner, C., K. A. Otte, and E. von Elert. 2021. Phenotypic convergence in a natural *Daphnia*
836 population acclimated to low temperature. Ecology and Evolution **11**: 15312–15324.
837 doi:10.1002/ece3.8217
838 Wersebe, M. J., and L. J. Weider. 2023. Resurrection genomics provides molecular and phenotypic
839 evidence of rapid adaptation to salinization in a keystone aquatic species. Proceedings of the
840 National Academy of Sciences **120**: e2217276120. doi:10.1073/pnas.2217276120
841 Wickham, H. 2016. ggplot2: Elegant graphics for data analysis, Springer-Verlag New York.

842 Yampolsky, L. Y., T. M. M. Schaer, and D. Ebert. 2014. Adaptive phenotypic plasticity and local
843 adaptation for temperature tolerance in freshwater zooplankton. Proc Biol Sci **281**:
844 20132744. doi:10.1098/rspb.2013.2744
845 Yousey, A. M., P. R. Chowdhury, N. Biddinger, J. H. Shaw, P. D. Jeyasingh, and L. J. Weider. 2018.
846 Resurrected 'ancient' *Daphnia* genotypes show reduced thermal stress tolerance compared
847 to modern descendants. Royal Society Open Science **5**: 172193. doi:10.1098/rsos.172193
848 Zeis, B. 2020. Hemoglobin in Arthropods—*Daphnia* as a Model, p. 163–194. *In* U. Hoeger and J.R.
849 Harris [eds.], Vertebrate and Invertebrate Respiratory Proteins, Lipoproteins and other Body
850 Fluid Proteins. Springer International Publishing.
851 Zeis, B., D. Becker, P. Gerke, M. Koch, and R. J. Paul. 2013. Hypoxia-inducible haemoglobins of
852 *Daphnia pulex* and their role in the response to acute and chronic temperature increase.
853 Biochimica et Biophysica Acta (BBA) - Proteins and Proteomics **1834**: 1704–1710.
854 doi:10.1016/j.bbapap.2013.01.036
855 Zeis, B., I. Buchen, A. Wacker, and D. Martin-Creuzburg. 2019. Temperature-induced changes in body
856 lipid composition affect vulnerability to oxidative stress in *Daphnia magna*. Comparative
857 Biochemistry and Physiology Part - B: Biochemistry and Molecular Biology **232**: 101–107.
858 doi:10.1016/j.cbpb.2019.03.008
859 Zeis, B., M. Koch, U. Gigengack, T. Morawe, and R. J. Paul. 2023. Limits of the thermal tolerance of
860 two lentic crustaceans: The role of lactate dehydrogenase. Journal of Experimental Zoology
861 Part A: Ecological and Integrative Physiology **339**: 565–577. doi:10.1002/jez.2700
862

Supplementary Material for

Impact of warming on functional traits of a keystone grazer in Arctic lakes

Athina Karapli-Petritsopoulou[1,2]*, Dörthe Becker[3], Dagmar Frisch[1]

[1] Department of Evolutionary and Integrative Ecology, Leibniz Institute of Freshwater Ecology and Inland Fisheries (IGB), Berlin, Germany

[2] Department of Biology, Chemistry, Pharmacy, Institute of Biology, Freie Universität Berlin, Berlin, Germany

[3] NABU-Naturschutzstation Niederrhein, Kleve, Germany

*Corresponding author: athena.karapli@igb-berlin.de

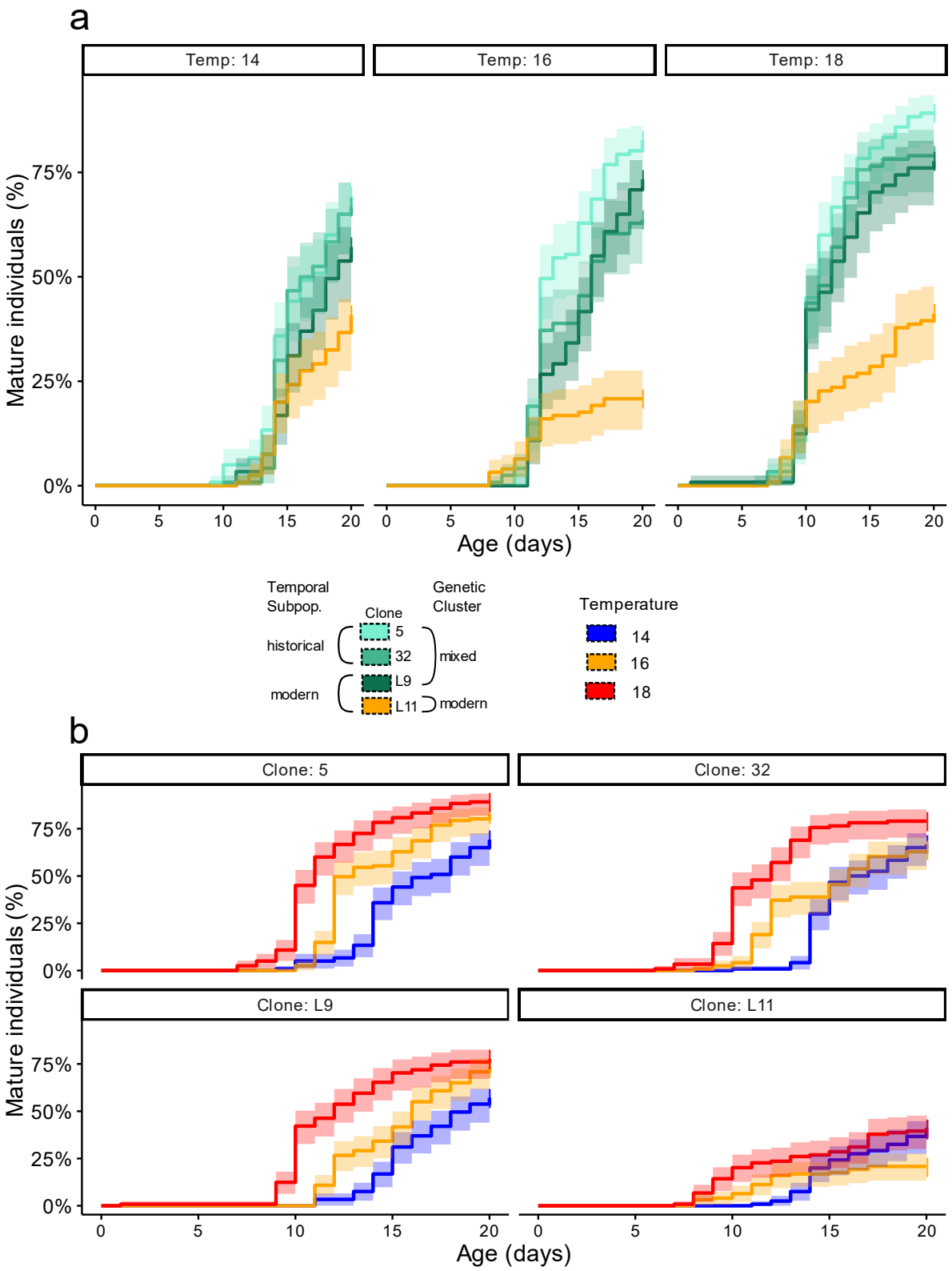

Figure S1. Kaplan-Meier curves for $Time_{mat}$ (here shown as age in days) of four clones across three temperatures. Note that the real age at maturity could be plus 1-2 days, as the experiment starts with up to 48h-old juveniles. Data are from animals from the physiological assays. Data are grouped by Temperature in panel a) and by Clone in panel b). Ribbons around curves show the 95% Confidence intervals.

Table S1. Model Comparison results for the relative oxygenated Haemoglobin peak at 576 nm ($rPeak_{576}$) (a.), TBARS (b.), GST activity (c.), Growth rate to Maturity (GR_{mat}) (d.), Size at Maturity ($Size_{mat}$) (e.), and Time to Maturity ($Time_{mat}$) (f.). Significant p-values ($p < 0.05$) and chosen models are in bold.

a. $rPeak_{576}$

$modrP_{576}$ 0: log($rPeak_{576}$) ~ 1 + (1 | Batch)

$modrP_{576}$ 1: log($rPeak_{576}$) ~ 1 + Temperature + (1 | Batch)

$modrP_{576}$ 2: log($rPeak_{576}$) ~ 1 + Temperature + Clone + (1 | Batch)

$modrP_{576}$ 3: log($rPeak_{576}$) ~ 1 + Temperature + Clone + Nr.animals with eggs + (1 | Batch)

$modrP_{576}$ 4: log($rPeak_{576}$) ~ 1 + Temperature + Clone + Nr.animals with eggs + Nr. animals with ephippia + (1 | Batch)

$modrP_{576}$ 5: log($rPeak_{576}$) ~ 1 + Temp + Clone + Temp:Clone + Nr.animals with eggs + Nr. animals with ephippia + (1 | Batch)

	npar	AIC	BIC	logLik	-2log(L)	Chisq	df	P p-value
$modrP_{576}$ 0	3	22.82	28.31	-8.41	16.82			
$modrP_{576}$ 1	5	25.30	34.44	-7.65	15.30	1.52	2	0.468
$modrP_{576}$ 2	8	-6.53	8.10	11.27	-22.53	37.83	3	**3.07E-08**
$modrP_{576}$ 3	9	-4.99	11.46	11.50	-22.99	0.46	1	0.497
$modrP_{576}$ 4	10	-3.11	15.18	11.55	-23.11	0.11	1	0.737
$modrP_{576}$ 5	16	3.17	32.43	14.41	-28.83	5.72	6	0.455

b. TBARS

modTBARS 0: log(TBARS) ~ 1 + (1 | Batch)

modTBARS 1: log(TBARS) ~ 1 + Temperature + (1 | Batch)

modTBARS 2: log(TBARS) ~ 1 + Temperature + Clone + (1 | Batch)

modTBARS 3: log(TBARS) ~ 1 + Temperature + Clone + Nr.animals with eggs + (1 | Batch)

modTBARS 4: log(TBARS) ~ 1 + Temperature + Clone + Nr.animals with eggs + Nr. animals with ephippia + (1 | Batch)

modTBARS 5: log(TBARS) ~ 1 + Temp + Clone + Temp:Clone + Nr.animals with eggs + Nr. animals with ephippia + (1 | Batch)

	npar	AIC	BIC	logLik	-2log(L)	Chisq	df	P p-value
modTBARS 0	3	32.95	38.43	-13.47	26.95			
modTBARS 1	5	33.22	42.36	-11.61	23.22	3.73	2	0.16
modTBARS 2	8	29.00	43.62	-6.50	13.00	10.23	3	**0.02**
modTBARS 3	9	26.30	42.76	-4.15	8.30	4.69	1	**0.03**
modTBARS 4	10	26.87	45.16	-3.44	6.87	1.43	1	0.23
modTBARS 5	16	34.88	64.14	-1.44	2.88	3.99	6	0.68

c. GST activity

modGST 0: log(GST activity) ~ 1 + (1 | Batch)

modGST 1: log(GST activity) ~ 1 + Temperature + (1 | Batch)

modGST 2: log(GST activity) ~ 1 + Temperature + Clone + (1 | Batch)

modGST 3: log(GST activity) ~ 1 + Temperature + Clone + Nr.animals with eggs + (1 | Batch)

modGST 4: log(GST activity) ~ 1 + Temperature + Clone + Nr.animals with eggs + Nr. animals with ephippia + (1 | Batch)

modGST 5: log(GST activity) ~ 1 + Temp + Clone + Temp:Clone + Nr.animals with eggs + Nr. animals with ephippia + (1 | Batch)

	npar	AIC	BIC	logLik	-2log(L)	Chisq	df	P p-value
modGST 0	3	29.18	34.66	-11.59	23.18			
modGST 1	5	31.89	41.03	-10.94	21.89	1.29	2	0.525
modGST 2	8	34.57	49.20	-9.28	18.57	3.32	3	0.345
modGST 3	9	35.74	52.20	-8.87	17.74	0.83	1	0.362
modGST 4	10	37.69	55.98	-8.85	17.69	0.05	1	0.831
modGST 5	16	46.67	75.93	-7.34	14.67	3.02	6	0.806

d. GR_{mat}

modGrMat 0: GR_{mat} ~ 1 + (1 | Clone:Block)

modGrMat 1: GR_{mat} ~ 1 + Temperature + (1 | Clone:Block)

modGrMat 2: GR_{mat} ~ 1 + Temperature + Clone + (1 | Clone:Block)

modGrMat 3: GR_{mat} ~ 1 + Temperature + Clone + Temperature:Clone + (1 | Clone:Block)

	npar	AIC	BIC	logLik	-2log(L)	Chisq	df	P p-value
modGrMat 0	3	2470.8	2481.7	-1232.4	2464.8			
modGrMat 1	5	2357	2375.1	-1173.5	2347	117.87	2	**< 2.2e-16**
modGrMat 2	8	2335.3	2364.3	-1159.7	2319.3	27.66	3	**4.27E-06**
modGrMat 3	14	2331.7	2382.6	-1151.9	2303.7	15.56	6	**0.016**

e. $Size_{mat}$

modSzMat 0: $Size_{mat}$ ~ 1 + (1 | Clone:Block)

modSzMat 1: $Size_{mat}$ ~ 1 + Temperature + (1 |Clone:Block)

modSzMat 2: $Size_{mat}$ ~ 1 + Temperature + Clone + (1 | Clone:Block)

modSzMat 3: $Size_{mat}$ ~ 1 + Temperature + Clone + Temperature:Clone + (1 | Clone:Block)

	npar	AIC	BIC	logLik	-2log(L)	Chisq	df	P p-value
modSzMat 0	3	3515.5	3526.4	-1754.8	3509.5			
modSzMat 1	5	3510.9	3529.1	-1750.5	3500.9	8.56	2	**0.014**
modSzMat 2	8	3500.2	3529.2	-1742.1	3484.2	16.74	3	**0.001**
modSzMat 3	14	3505.9	3556.8	-1739	3477.9	6.27	6	0.393

f. $Time_{mat}$

ModTMat 1: Surv($Time_{mat}$, status) ~ Temperature:strata(t) + Clone:strata(t) + frailty(Block)

ModTMat 2: Surv($Time_{mat}$, status) ~ Temperature:strata(t) + Clone:strata(t) + Temperature:Clone + frailty(Block)

	loglik	Chisq	df	p-value
ModTMat 1	-1199.7			
ModTMat 2	-1196.1	7.23	4.22	0.141

Table S2. Extended results for the relative oxygenated Haemoglobin peak at 576 nm. Estimates from Linear mixed model fit by REML. t-tests use Satterthwaite's method (a). Post-hoc contrasts on estimated marginal means (EMMs) with Holm correction. Contrasts between Temperature levels are averaged for Clone (b) and contrasts between Clones are averaged for Temperature (c). Cohen's d for EMMs contrasts (d). Significant p-values ($p < 0.05$) and substantial effect sizes with 95% Confidence intervals (CI) not including 0 are in bold.

Chosen model: log(rPeak576) ~ 1 + Temp + Clone + (1 | Batch)

a.

	Estimate	Std. Error	df	t value	p-value
(Intercept)	**-5.79**	0.11	5.82	-52.66	**5.09E-09**
Temp16	0.11	0.07	37.02	1.60	0.118
Temp18	0.10	0.07	37.02	1.52	0.136
Clone32	-0.03	0.07	37.00	-0.41	0.682
CloneL9	-0.14	0.08	37.02	-1.84	0.074
CloneL11	**0.40**	0.08	37.02	5.21	**7.42E-06**

b.

contrast	Estimate	SE	df	lower CI	upper CI	t ratio	p-value
Temp14 - Temp16	-0.11	0.07	37	-0.27	0.06	-1.60	0.353
Temp14 - Temp18	-0.10	0.07	37	-0.27	0.06	-1.52	0.353
Temp16 - Temp18	0.01	0.07	37	-0.16	0.17	0.08	0.938

c.

contrast	Estimate	SE	df	lower CI	upper CI	t ratio	p-value
Clone 5 - Clone 32	0.03	0.07	37	-0.18	0.24	0.41	0.682
Clone 5 - Clone L9	0.14	0.08	37	-0.07	0.35	1.84	0.221
Clone 5 - Clone L11	-0.40	0.08	37	-0.61	-0.19	-5.21	**<.0001**
Clone 32 - Clone L9	0.11	0.08	37	-0.10	0.32	1.44	0.318
Clone 32 - Clone L11	-0.43	0.08	37	-0.64	-0.22	-5.61	**<.0001**
Clone L9 - Clone L11	-0.54	0.08	37	-0.76	-0.32	-6.86	**<.0001**

d.

Contrast	Effect size	SE	df	lower CI	upper CI
Temp14 - Temp16	-0.41	0.26	4.01	-1.14	0.32
Temp14 - Temp18	-0.39	0.26	4.01	-1.12	0.34
Temp16 - Temp18	0.02	0.26	4.13	-0.70	0.74

Contrast	Effect size	SE	df	lower CI	upper CI
Clone 5 - Clone 32	0.12	0.29	4.57	-0.65	0.90
Clone 5 - Clone L9	0.55	0.31	4.57	-0.26	1.36
Clone 5 - Clone L11	**-1.56**	0.35	4.57	**-2.49**	**-0.63**
Clone 32 - Clone L9	0.43	0.30	4.57	-0.37	1.24
Clone 32 - Clone L11	**-1.68**	0.36	4.57	**-2.63**	**-0.74**
Clone L9 - Clone L11	**-2.11**	0.39	4.81	**-3.14**	**-1.09**

Table S3. Extended results for TBARS. Estimates from Linear mixed model fit by REML. t-tests use Satterthwaite's method (a). Post-hoc contrasts on estimated marginal means (EMMs) with Holm correction. Contrasts between Temperature levels are averaged for Clone (b) and contrasts between Clones are averaged for Temperature (c). Cohen's d for EMMs contrasts (d). Significant p-values ($p < 0.05$) and substantial effect sizes with 95% Confidence intervals (CI) not including 0 are in bold.

Chosen model: log(TBARS) ~ 1 + Temperature + Clone + Nr.animals with eggs + (1 | Batch)

a.

	Estimate	Std. Error	df	t value	p-value
Intercept	0.46	0.26	38.96	1.76	0.086
Temp16	0.27	0.10	35.94	2.67	**0.011**
Temp18	0.13	0.10	36.01	1.28	0.209
Clone32	0.05	0.13	36.32	0.37	0.713
CloneL9	0.02	0.12	36.05	0.17	0.867
CloneL11	0.59	0.19	36.71	3.09	**0.004**
Nr.animals with eggs	0.01	0.00	37.49	2.04	**0.048**

b.

Contrast	Estimate	SE	df	lower CI	upper CI	t ratio	p-value
Temp14 - Temp16	-0.27	0.10	36	-0.52	-0.02	-2.67	**0.034**
Temp14 - Temp18	-0.13	0.10	36.1	-0.38	0.12	-1.28	0.353
Temp16 - Temp18	0.14	0.10	36.2	-0.12	0.39	1.38	0.353

c.

Contrast	Estimate	SE	df	lower CI	upper CI	t ratio	p-value
Clone 5 - Clone 32	-0.05	0.13	36.40	-0.41	0.31	-0.37	1
Clone 5 - Clone L9	-0.02	0.12	36.10	-0.35	0.31	-0.17	1
Clone 5 - Clone L11	-0.59	0.19	36.80	-1.12	-0.05	-3.06	**0.016**
Clone 32 - Clone L9	0.03	0.12	36.30	-0.31	0.37	0.23	1
Clone 32 - Clone L11	-0.54	0.15	36.40	-0.95	-0.13	-3.69	**0.004**
Clone L9 - Clone L11	-0.57	0.18	36.80	-1.06	-0.07	-3.21	**0.014**

d.

Contrast	Effect size	SE	df	lower CI	upper CI
Temp14 - Temp16	**-0.91**	0.36	8.34	**-1.73**	**-0.09**
Temp14 - Temp18	-0.44	0.35	8.34	-1.23	0.35
Temp16 - Temp18	0.47	0.35	8.95	-0.32	1.26

Contrast	Effect size	SE	df	lower CI	upper CI
Clone 5 - Clone 32	-0.16	0.44	11.50	-1.12	0.80
Clone 5 - Clone L9	-0.07	0.40	15.20	-0.92	0.78
Clone 5 - Clone L11	**-1.99**	0.69	17.90	**-3.43**	**-0.54**
Clone 32 - Clone L9	0.09	0.42	11.50	-0.82	1.01
Clone 32 - Clone L11	**-1.82**	0.54	11.50	**-3.01**	**-0.64**
Clone L9 - Clone L11	**-1.92**	0.64	15.20	**-3.28**	**-0.56**

Table S4. Extended results for Growth rate to maturity (GR_{mat}). Estimates from Linear mixed model fit by REML. t-tests use Satterthwaite's method (a). Post-hoc contrasts on estimated marginal means (EMMs) with Holm correction. Contrasts between Temperature levels are averaged for Clone (b) and contrasts between Clones are averaged for Temperature (c). Cohen's d for EMMs contrasts (d). Significant p-values ($p < 0.05$) and substantial effect sizes with 95% Confidence intervals (CI) not including 0 are in bold.

Chosen model: GR_{mat} ~ 1 + Temperature + Clone + Temperature:Clone + (1 | Clone:Block)

a.

	Estimate	Std. Error	df	t value	p-value
Intercept	64.47	4.64	45.49	13.90	**< 2e-16**
Temp16	18.71	5.01	247.76	3.73	**2.34E-04**
Temp18	34.13	5.02	255.39	6.80	**7.29E-11**
Clone32	-1.08	6.45	49.61	-0.17	0.867
CloneL9	7.55	6.64	42.65	1.14	0.262
CloneL11	-15.16	6.58	45.34	-2.30	**0.026**
Temp16:Clone32	-8.68	7.28	212.67	-1.19	0.234
Temp18:Clone32	0.89	7.23	225.35	0.12	0.902
Temp16:CloneL9	-8.45	7.44	241.98	-1.14	0.258
Temp18:CloneL9	1.36	6.79	264.14	0.20	0.842
Temp16:CloneL11	-18.92	7.59	222.49	-2.49	**0.013**
Temp18:CloneL11	-17.89	6.84	263.24	-2.61	**0.009**

b.

Within Clone 5

contrast	Estimate	SE	df	lower CI	upper CI	t ratio	p-value
Temp14 - Temp16	-18.71	5.07	250	-30.9	-6.49	-3.69	**0.001**
Temp14 - Temp18	-34.13	5.07	257	-46.4	-21.91	-6.73	**<.0001**
Temp16 - Temp18	-15.42	4.47	263	-26.2	-4.64	-3.45	**0.001**

Within Clone 32

contrast	Estimate	SE	df	lower CI	upper CI	t ratio	p-value
Temp14 - Temp16	-10.03	5.37	185	-23	2.94	-1.87	0.063
Temp14 - Temp18	-35.02	5.28	198	-47.8	-22.27	-6.63	**<.0001**
Temp16 - Temp18	-24.99	5.37	188	-38	-12.01	-4.65	**<.0001**

Within Clone L9

contrast	Estimate	SE	df	lower CI	upper CI	t ratio	p-value
Temp14 - Temp16	-10.27	5.57	240	-23.7	3.17	-1.84	0.067
Temp14 - Temp18	-35.49	4.61	267	-46.6	-24.39	-7.70	**<.0001**
Temp16 - Temp18	-25.22	5.24	265	-37.8	-12.61	-4.82	**<.0001**

Within Clone L11

contrast	Estimate	SE	df	lower CI	upper CI	t ratio	p-value
Temp14 - Temp16	0.21	5.78	207	-13.7	14.17	0.04	0.971
Temp14 - Temp18	-16.24	4.69	267	-27.5	-4.95	-3.47	**0.002**
Temp16 - Temp18	-16.45	5.69	230	-30.2	-2.74	-2.89	**0.008**

c.

Within Temperature 14

contrast	Estimate	SE	df	lower CI	upper CI	t ratio	p-value
Clone 5 - Clone 32	1.08	6.49	55.1	-16.67	18.84	0.17	0.868
Clone 5 - Clone L9	-7.55	6.66	47.5	-25.89	10.79	-1.13	0.583
Clone 5 - Clone L11	15.16	6.6	50.5	-2.97	33.29	2.30	0.129
Clone 32 - Clone L9	-8.64	6.57	51.4	-26.66	9.38	-1.32	0.583
Clone 32 - Clone L11	14.08	6.51	54.9	-3.73	31.89	2.16	0.140
Clone L9 - Clone L11	22.71	6.68	47.4	4.31	41.11	3.40	**0.008**

Within Temperature 16

contrast	Estimate	SE	df	lower CI	upper CI	t ratio	p-value
Clone 5 - Clone 32	9.77	6.53	54.8	-8.11	27.64	1.50	0.421
Clone 5 - Clone L9	0.90	7.1	54.8	-18.54	20.33	0.13	0.900
Clone 5 - Clone L11	34.08	7.07	56	14.74	53.42	4.82	**1.00E-04**
Clone 32 - Clone L9	-8.87	7.03	59	-28.07	10.32	-1.26	0.424
Clone 32 - Clone L11	24.32	7	60.3	5.22	43.42	3.47	**0.004**
Clone L9 - Clone L11	33.19	7.54	59.5	12.62	53.76	4.40	**2.00E-04**

Within Temperature 18

contrast	Estimate	SE	df	lower CI	upper CI	t ratio	p-value
Clone 5 - Clone 32	0.20	6.6	57.7	-17.84	18.23	0.03	0.976
Clone 5 - Clone L9	-8.91	6.88	51.4	-27.77	9.96	-1.30	0.540
Clone 5 - Clone L11	33.05	6.85	55.3	14.32	51.79	4.83	**<.0001**
Clone 32 - Clone L9	-9.10	6.7	55	-27.45	9.24	-1.36	0.540
Clone 32 - Clone L11	32.85	6.67	59.6	14.64	51.06	4.92	**<.0001**
Clone L9 - Clone L11	41.96	6.94	53	22.92	60.99	6.04	**<.0001**

d.

Within Clone 5

Contrast	Effect size	SE	df	lower CI	upper CI
Temp14 - Temp16	**-1.11**	0.32	250.00	**-1.74**	**-0.47**
Temp14 - Temp18	**-2.02**	0.37	257.00	**-2.75**	**-1.29**
Temp16 - Temp18	**-0.91**	0.28	263.00	**-1.47**	**-0.36**

Within Clone 32

Contrast	Effect size	SE	df	lower CI	upper CI
Temp14 - Temp16	-0.59	0.32	185.00	-1.23	0.05
Temp14 - Temp18	**-2.07**	0.39	198.00	**-2.83**	**-1.31**
Temp16 - Temp18	**-1.48**	0.36	188.00	**-2.18**	**-0.78**

Within Clone L9

Contrast	Effect size	SE	df	lower CI	upper CI
Temp14 - Temp16	-0.61	0.34	240.00	-1.27	0.05
Temp14 - Temp18	**-2.10**	0.36	267.00	**-2.80**	**-1.40**
Temp16 - Temp18	**-1.49**	0.35	265.00	**-2.18**	**-0.80**

Within Clone L11

Contrast	Effect size	SE	df	lower CI	upper CI
Temp14 - Temp16	0.01	0.34	207.00	-0.66	0.69
Temp14 - Temp18	**-0.96**	0.30	267.00	**-1.54**	**-0.38**
Temp16 - Temp18	**-0.97**	0.35	230.00	**-1.67**	**-0.28**

Within Temperature 14

Contrast	Effect size	SE	df	lower CI	upper CI
Clone 5 - Clone 32	0.06	0.38	55.10	-0.71	0.83
Clone 5 - Clone L9	-0.45	0.40	47.50	-1.24	0.35
Clone 5 - Clone L11	**0.90**	0.40	50.50	**0.09**	**1.70**
Clone 32 - Clone L9	-0.51	0.39	51.40	-1.30	0.28
Clone 32 - Clone L11	**0.83**	0.39	54.90	**0.04**	**1.62**
Clone L9 - Clone L11	**1.34**	0.42	47.40	**0.50**	**2.19**

Within Temperature 16

Contrast	Effect size	SE	df	lower CI	upper CI
Clone 5 - Clone 32	0.58	0.39	54.80	-0.21	1.36
Clone 5 - Clone L9	0.05	0.42	54.80	-0.79	0.90
Clone 5 - Clone L11	**2.02**	0.47	56.00	**1.08**	**2.95**
Clone 32 - Clone L9	-0.53	0.42	59.00	-1.36	0.31
Clone 32 - Clone L11	**1.44**	0.44	60.30	**0.56**	**2.32**
Clone L9 - Clone L11	**1.96**	0.49	59.50	**0.98**	**2.94**

Within Temperature 18

Contrast	Effect size	SE	df	lower CI	upper CI
Clone 5 - Clone 32	0.01	0.39	57.70	-0.77	0.79
Clone 5 - Clone L9	-0.53	0.41	51.40	-1.35	0.30
Clone 5 - Clone L11	**1.96**	0.45	55.30	**1.05**	**2.86**
Clone 32 - Clone L9	-0.54	0.40	55.00	-1.34	0.26
Clone 32 - Clone L11	**1.94**	0.44	59.60	**1.06**	**2.83**
Clone L9 - Clone L11	**2.48**	0.48	53.00	**1.51**	**3.45**

Table S5. Extended results for $Size_{mat}$. Estimates from Linear mixed model fit by REML. t-tests use Satterthwaite's method (a). Post-hoc contrasts on estimated marginal means (EMMs) with Holm correction. Contrasts between Temperature levels are averaged for Clone (b) and contrasts between Clones are averaged for Temperature (c). Cohen's d for EMMs contrasts (d). Significant p-values ($p < 0.05$) and substantial effect sizes with 95% Confidence intervals (CI) not including 0 are in bold.

Chosen model: $Size_{mat}$ ~ 1 + Temperature + Clone + (1 | Clone:Block)

a.

	Estimate	Std. Error	df	t value	p-value
Intercept	1991.44	28.64	29.50	69.53	**< 2e-16**
Temp16	-4.74	21.32	201.09	-0.22	0.824
Temp18	-49.30	19.67	251.12	-2.51	**0.013**
Clone32	-0.87	35.63	24.86	-0.02	0.981
CloneL9	-22.17	38.81	22.68	-0.57	0.573
CloneL11	128.68	38.05	23.87	3.38	**0.002**

b.

contrast	Estimate	SE	df	lower CI	upper CI	t ratio	p-value
Temp14 - Temp16	4.74	21.6	209	-47.41	56.9	0.22	0.827
Temp14 - Temp18	49.3	19.9	254	1.4	97.2	2.48	**0.041**
Temp16 - Temp18	44.56	20.8	249	-5.48	94.6	2.15	0.066

c.

contrast	Estimate	SE	df	lower CI	upper CI	t ratio	p-value
Clone 5 - Clone 32	0.87	35.7	28.4	-100.3	102	0.02	1
Clone 5 - Clone L9	22.17	38.9	26	-88.8	133.2	0.57	1
Clone 5 - Clone L11	-128.68	38.1	27.3	-237.1	-20.2	-3.38	**0.009**
Clone 32 - Clone L9	21.30	37.1	28.3	-84.1	126.7	0.57	1
Clone 32 - Clone L11	-129.55	36.4	30.1	-232.2	-26.9	-3.56	**0.006**
Clone L9 - Clone L11	-150.85	39.5	27.2	-263.2	-38.5	-3.82	**0.004**

d.

Contrast	Effect size	SE	df	lower CI	upper CI
Temp14 - Temp16	0.04	0.16	59.80	-0.29	0.36
Temp14 - Temp18	**0.37**	0.16	59.80	**0.06**	**0.68**
Temp16 - Temp18	**0.33**	0.16	63.80	**0.01**	**0.65**

Contrast	Effect size	SE	df	lower CI	upper CI
Clone 5 - Clone 32	0.01	0.27	25.90	-0.54	0.56
Clone 5 - Clone L9	0.17	0.29	25.90	-0.43	0.77
Clone 5 - Clone L11	**-0.97**	0.29	25.90	**-1.56**	**-0.37**
Clone 32 - Clone L9	0.16	0.28	26.00	-0.41	0.73
Clone 32 - Clone L11	**-0.97**	0.28	28.70	**-1.54**	**-0.41**
Clone L9 - Clone L11	**-1.13**	0.30	26.00	**-1.75**	**-0.51**

Table S6. Extended Cox PH model results for $Time_{mat}$ and Post-hoc contrasts of estimated marginal means for fitness mode animals. (a) Coefficients estimated from Cox PH model, where coefficient is the logarithm of the Hazard ratio, reference groups are Clone 5 and Temperature 18, SE: standard error, HR: Hazard ratio, CI: confidence interval. (b) Post-hoc contrasts of estimated marginal means calculated using the model coefficients, with Holm correction. Estimated from a model with Block as a fixed term. Contrasts between Temperature levels are averaged for Clone and (c) contrasts between Clones are averaged for Temperature. Significant p-values ($p < 0.05$) are in bold.

a. Chosen model: Surv($Time_{mat}$, status) ~ Temp:strata(t) + Clone:strata(t) +frailty(Block)

	Coefficient (SE)	HR [95% CI]	p-value
frailty(Block)			0.110
Temp14:strata(t)t=1	-3.01 (0.36)	0.05 [0.02,0.10]	**9.2E-17**
Temp16:strata(t)t=1	-1.38 (0.22)	0.25 [0.16,0.38]	**1.8E-10**
Temp14:strata(t)t=2	-0.73 (0.36)	0.48 [0.24,0.97]	**0.041**
Temp16:strata(t)t=2	-0.88 (0.38)	0.41 [0.20,0.87]	**0.019**
Temp14:strata(t)t=3	-1.29 (0.66)	0.28 [0.08,1.00]	0.050
Temp16:strata(t)t=3	-0.93 (0.64)	0.40 [0.11,1.39]	0.150
Temp14:strata(t)t=4	0.05 (0.53)	1.05 [0.37,2.93]	0.93
Temp16:strata(t)t=4	0.34 (0.54)	1.40 [0.48,4.05]	0.53
strata(t)t=1:Clone32	-0.20 (0.25)	0.82 [0.50,1.33]	0.42
strata(t)t=2:Clone32	-0.24 (0.27)	0.78 [0.46,1.34]	0.38
strata(t)t=3:Clone32	-0.36 (0.59)	0.70 [0.22,2.21]	0.54
strata(t)t=4:Clone32	0.57 (0.69)	1.77 [0.46,6.83]	0.41
strata(t)t=1:CloneL9	0.16 (0.26)	1.17 [0.71,1.94]	0.53
strata(t)t=2:CloneL9	-0.35 (0.31)	0.71 [0.39,1.29]	0.26
strata(t)t=3:CloneL9	0.23 (0.58)	1.26 [0.41,3.91]	0.69
strata(t)t=4:CloneL9	-1.56 (0.92)	0.21 [0.03,1.26]	0.09
strata(t)t=1:CloneL11	-1.77 (0.37)	0.17 [0.08,0.36]	**2.3E-06**
strata(t)t=2:CloneL11	-1.64 (0.35)	0.19 [0.10,0.39]	**2.6E-06**
strata(t)t=3:CloneL11	-1.52 (0.61)	0.22 [0.07,0.72]	**0.01**
strata(t)t=4:CloneL11	-1.03 (0.61)	0.36 [0.11,1.17]	0.09

b. Post-hoc contrasts of estimated marginal means between Temperatures for each time period (t)

For time period (t) 1 [0, 14 days]

Contrast	Estimate	SE	95% CI	z-ratio	p.value
Temp14 - Temp16	-1.59	0.38	(-2.82,-0.36)	-4.24	**0.001**
Temp14 - Temp18	-3.07	0.36	(-4.24,-1.89)	-8.50	**<.0001**
Temp16 - Temp18	-1.47	0.22	(-2.18,-0.76)	-6.78	**<.0001**

For time period (t) 2 [15, 20 days]

Contrast	Estimate	SE	95% CI	z-ratio	p-value
Temp14 - Temp16	0.20	0.24	(-0.58,0.98)	0.82	1.000
Temp14 - Temp18	-0.71	0.36	(-1.89,0.46)	-1.98	0.705
Temp16 - Temp18	-0.91	0.38	(-2.16,0.34)	-2.38	0.420

For time period (t) 3 [21, 25 days]

Contrast	Estimate	SE	95% CI	z-ratio	p-value
Temp14 - Temp16	-0.28	0.42	(-1.64,1.08)	-0.67	1.000
Temp14 - Temp18	-1.12	0.65	(-3.23,0.98)	-1.74	0.849
Temp16 - Temp18	-0.85	0.64	(-2.93,1.24)	-1.33	0.976

For time period (t) 4 > 25 days

Contrast	Estimate	SE	95% CI	z-ratio	p-value
Temp14 - Temp16	-0.27	0.40	(-1.56,1.02)	-0.69	1.000
Temp14 - Temp18	0.26	0.50	(-1.37,1.88)	0.51	1.000
Temp16 - Temp18	0.53	0.52	(-1.18,2.23)	1.01	0.998

c. Post-hoc contrasts of estimated marginal means between Clones for each time period (t)

For time period (t) 1 [0, 14 days]

Contrast	Estimate	SE	95% CI	z-ratio	p-value
Clone 5 - Clone 32	0.28	0.24	(-0.61,1.16)	1.14	1.000
Clone 5 - Clone L9	-0.06	0.24	(-0.94,0.82)	-0.25	1.000
Clone 5 - Clone L11	1.75	0.37	(0.42,3.08)	4.78	**0.001**
Clone 32 - Clone L9	-0.34	0.24	(-1.22,0.55)	-1.38	1.000
Clone 32 - Clone L11	1.47	0.37	(0.13,2.81)	3.98	**0.015**
Clone L9 - Clone L11	1.81	0.38	(0.44,3.17)	4.82	**4.E-04**

For time period (t) 2 [15, 20 days]

Contrast	Estimate	SE	95% CI	z-ratio	p-value
Clone 5 - Clone 32	0.23	0.27	(-0.75,1.21)	0.86	1.000
Clone 5 - Clone L9	0.43	0.30	(-0.67,1.53)	1.42	0.999
Clone 5 - Clone L11	1.52	0.35	(0.24,2.79)	4.31	**0.004**
Clone 32 - Clone L9	0.20	0.30	(-0.91,1.30)	0.65	1.000
Clone 32 - Clone L11	1.28	0.35	(0.00,2.57)	3.65	**0.049**
Clone L9 - Clone L11	1.09	0.39	(-0.31,2.49)	2.82	0.420

For time period (t) 3 [21, 25 days]

Contrast	Estimate	SE	95% CI	z-ratio	p-value
Clone 5 - Clone 32	0.38	0.59	(-1.75,2.52)	0.65	1.000
Clone 5 - Clone L9	-0.09	0.58	(-2.20,2.02)	-0.15	1.000
Clone 5 - Clone L11	1.39	0.61	(-0.82,3.59)	2.29	0.823
Clone 32 - Clone L9	-0.47	0.53	(-2.40,1.45)	-0.89	1.000
Clone 32 - Clone L11	1.00	0.56	(-1.03,3.04)	1.79	0.985
Clone L9 - Clone L11	1.47	0.57	(-0.58,3.53)	2.61	0.589

For time period (t) 4 > 25 days

Contrast	Estimate	SE	95% CI	z-ratio	p-value
Clone 5 - Clone 32	-0.56	0.69	(-3.06,1.94)	-0.82	1.000
Clone 5 - Clone L9	1.69	0.90	(-1.59,4.96)	1.87	0.974
Clone 5 - Clone L11	0.87	0.59	(-1.27,3.00)	1.48	0.999
Clone 32 - Clone L9	2.25	0.82	(-0.72,5.22)	2.75	0.473
Clone 32 - Clone L11	1.43	0.51	(-0.44,3.30)	2.78	0.455
Clone L9 - Clone L11	-0.82	0.68	(-3.30,1.66)	-1.20	1.000